



All Theses and Dissertations

2018-03-01

Mechanical Properties of Inconel 718 Processed Using Electron Beam Free Form Fabrication (EBF³)

Brent R. Waters
Brigham Young University

Follow this and additional works at: <https://scholarsarchive.byu.edu/etd>

 Part of the [Construction Engineering and Management Commons](#)

BYU ScholarsArchive Citation

Waters, Brent R., "Mechanical Properties of Inconel 718 Processed Using Electron Beam Free Form Fabrication (EBF³)" (2018). *All Theses and Dissertations*. 6717.

<https://scholarsarchive.byu.edu/etd/6717>

This Thesis is brought to you for free and open access by BYU ScholarsArchive. It has been accepted for inclusion in All Theses and Dissertations by an authorized administrator of BYU ScholarsArchive. For more information, please contact scholarsarchive@byu.edu, ellen_amatangelo@byu.edu.

Mechanical Properties of Inconel 718 Processed Using
Electron Beam Free Form Fabrication
(EBF³)

Brent R. Waters

A thesis submitted to the faculty of
Brigham Young University
in partial fulfillment of the requirements for the degree of
Master of Science

Michael P. Miles, Chair
David T. Fullwood
Jason M. Weaver

School of Technology
Brigham Young University

Copyright © 2018 Brent R. Waters

All Rights Reserved

ABSTRACT

Mechanical Properties of Inconel 718 Processed Using Electron Beam Free Form Fabrication (EBF³)

Brent R. Waters
School of Technology, BYU
Master of Science

Electron beam freeform fabrication (EBF³) is a rapid metal deposition process that works efficiently with the weldable alloy Inconel 718 (IN 718). EBF³ is a developing additive manufacturing (AM) process that can manufacture IN 718 parts directly from computer aided design (CAD) data. EBF³ can produce parts significantly faster and more energy efficient than competing IN 718 AM technologies. The EBF³ process utilizes metal wire feedstock which is induced into a molten pool using a focused electron beam in a vacuum environment. This allows parts to be built layer by layer, creating intricate shapes that can be produced cheaper and faster than traditionally manufactured IN 718 parts. Furthermore, it allows traditionally manufactured parts to be modified as additional form is added to them using EBF³. Multiple industries rely on IN 718 parts and can utilize this technology including aerospace engineering, oil refinery, nuclear power generation, and food processing.

A main drawback of EBF³ is the lack of knowledge of the effect different EBF³ build techniques will have on the properties of the deposited materials. Most of the reliable data on the mechanical properties relate to a linear build-up strategy and focus on the mechanical properties in the deposition direction (DD). There is no data related to other build-up techniques such as rotation build-up or transitional builds from forged material to EBF³ material. Reliable data on the behavior and microstructure of EBF³ material in a direction other than the DD is also difficult to find. Previous studies showed build-up height influenced mechanical properties but its role is not fully understood yet.

This paper presents the mechanical properties and microstructure of an IN 718 plate built using a EBF³ rotational build-up strategy through utilizing a forged plug in the center. The tensile properties of samples at the transition from forged to EBF³ material showed higher ductility and reduced strength than pure EBF³ material. This is likely due the influence of the forge material in one half of the specimen. Samples taken at approximately 15 degree increments from 0 to 90 degrees rotation to the DD in the additive portion of the plate were subjected to tensile testing. Along the build height, or the transverse direction (TD), the lowest strength was demonstrated and the TD aligned strongly to a <001> texture. Samples 45 degrees to the DD showed the greatest strength due to their preference for aligning to a <111> texture. Samples low on the build height demonstrated a higher strength than those on the top and displayed grain structures along the TD which were long, linear, and narrow across multiple deposition layers.

Keywords: electron beam freeform fabrication, EBF³, IN 718, mechanical properties, texture

ACKNOWLEDGEMENTS

Foremost, I want to thank my wonderful chair and mentor, Dr. Mike Miles. Without his support, guidance, and expertise this thesis wouldn't be possible. I'd also like to thank Dr. David Fullwood, who helped lead the project and determine its scope. It is also important to recognize Lockheed Martin who provided the material for this study and Brigham Young University who provided the necessary equipment and facilities. I'd also like to thank the National Science Foundation, which was the source of funding for this project through award #0928923.

I'd like to thank everyone who helped this project progress. Without their help, the project never could have been a success. To name a few: Jason Weaver, Ruth Ann Lowe, Isaac Chelladurai, Landon Hansen, Paul Minson, Jill Wen, and Rene Kekoolani.

I want to thank my amazing parents Bob and Angie who have always believed in me and my siblings Lauren, Kirk, and Adrienne who encouraged me to finish. Thank you, as well, to my wonderful in-laws Carla and John who are a source of support and motivation. Thanks to Isa for helping with revisions. Also, I thank my lovely wife, Lauren, who has been a constant light and source of inspiration throughout this step of my life. Finally, I'd like to dedicate this thesis to our beautiful daughter, Opal, who continues to bring us joy and enrich our lives.

TABLE OF CONTENTS

TABLE OF CONTENTS.....	iv
LIST OF TABLES.....	vi
LIST OF FIGURES	vii
1 Introduction	1
1.1 Background	1
1.1.1 The EBF ³ Process	2
1.1.2 EBF ³ Application to IN 718.....	3
1.1.3 EBF ³ Build-up Strategies.....	3
1.2 Hypotheses	6
1.3 Significance of the Study	6
1.4 Delimitations	7
1.5 Definition of Abbreviations and Terms	7
2 Literature Review	10
2.1 Mechanical Properties of Traditional Manufactured IN 718	10
2.2 Mechanical Properties of AM Processes of IN 718	10
2.3 Electron Beam Welding Parameters	12
2.4 Mechanical Properties of IN 718 Processed by EBF ³	13
2.4.1 Part Build Parameters	14
2.4.2 Test Sample Parameters.....	18
2.4.3 Chemical Composition.....	21
2.4.4 Microstructure.....	22
2.4.5 Crystal Orientation.....	23
2.4.6 Heat Treatment.....	24
3 Methodology.....	28
3.1 Plate Build Parameters	28
3.2 Test Sample Parameters	30
3.2.1 Microscopy Preparation	31
3.2.2 Tensile Testing.....	33
3.3 H1: Height Location vs Tensile Strength.....	34
3.4 H2: Sample Orientation vs Tensile Strength.....	35
4 Results and Discussion	36

4.1	Raw Data Results	36
4.1.1	Plate Build Parameters	37
4.1.2	Test Sample Parameters	38
4.1.3	Chemical Composition.....	40
4.1.4	Microstructure.....	41
4.1.4.1	Microstructure Along the TD	42
4.1.4.2	Microstructure at the Transition Zone.....	47
4.1.4.3	Crystal Orientation	48
4.1.4.3.1	Crystal Orientation Effect on Mechanical Properties	50
5	Conclusions and Recommendations.....	52
5.1	H1: Height Location vs Tensile Strength.....	52
5.1.1	Tensile Testing.....	52
5.1.2	Microscopy	53
5.2	H2: Sample Orientation vs Tensile Strength.....	54
5.3	Closing Remarks	54
	References.....	55

LIST OF TABLES

Table 2-1: Tensile Properties of IN 718 with Respect to Orientation	10
Table 2-2: Comparison of AM of IN 718	12
Table 2-3: Typical Welding Parameters for IN 718	12
Table 2-4: Comparison of Manufacturing Processes of IN 718	13
Table 2-5: Height, Width, Length Definitions.....	15
Table 2-6: HxWxL of Each NASA Part	17
Table 2-7: Mechanical Properties of Build Parameters	18
Table 2-8: Sample Dimensions from Each NASA Part.....	19
Table 2-9: Mechanical Properties of Sample Parameters	20
Table 2-10: Chemical Composition of Each Build, Wire and Nominal	21
Table 2-11: E Value Dependence on Crystal Orientation of Ni	24
Table 2-12: HT Methods Conducted on NASA Block 1	25
Table 2-13: HT Method Effect on Build-up Height Strength.....	25
Table 2-14: HT 2 of IN 718 with Respect to Orientation	26
Table 3-1: Build Dimensions of IN 718 Plate	29
Table 3-2: Sample Regions and Orientations	31
Table 3-3: Tensile Test Sample Dimensions	33
Table 4-1: Tensile Test Results.....	36
Table 4-2: Interim vs Non-interim and Transitional Properties.....	37
Table 4-3: Strength vs Wire Diameter	38
Table 4-4: Mechanical Properties of Plate Test Sample Parameters	39
Table 4-5: Microscopy Labels Matched to Plate Surface Orientations	41

LIST OF FIGURES

Figure 1-1: Electron Beam Freeform Fabrication System	2
Figure 1-2: IN 718 Fabricated Part Using a Linear EBF ³ Build-up	4
Figure 1-3: Inconel 718 Plate with Respective Orientation Labels	5
Figure 2-1: A Typical EBF ³ Set-up Used on IN 718	15
Figure 2-2: NASA Wall 1 (Left) and NASA Wall 2 (Right).....	16
Figure 2-3: NASA Block 1	16
Figure 2-4: NASA Block 2	17
Figure 2-5: ASTM E8 Standard for Subsize Tensile Specimen (in)	20
Figure 2-6: Typical EBF ³ Dendritic Structure on NASA Wall 2	22
Figure 2-7: NASA Block 2 at 0.4 and 0.9 Inch Build Height.....	23
Figure 2-8: Microstructure of As-Deposited and HT	26
Figure 2-9: Microhardness Evaluation of Crystal Anisotropy.....	27
Figure 3-1: IN 718 Plate Fabrication Details.....	29
Figure 3-2: Areas of Sample Removal and Microscopy Analysis.....	30
Figure 3-3: Surface Orientations Cut from Each Sample	31
Figure 3-4: Sample Orientations Mounted in Puck	32
Figure 3-5: Location of Dogbones Cut from Each Sample	33
Figure 3-6: Dogbone Dimensions Used for Tensile Testing (mm)	34
Figure 4-1: Stress/Strain Curve of Each Sample	40
Figure 4-2: Grain Size and Shape at 0, 45, and 90 Degrees to DD	43
Figure 4-3: Each Surface Orientation at the Inner Plate Area	44
Figure 4-4: Each Surface Orientation at the Middle Plate Area	45

Figure 4-5: Each Surface Orientation at the Outer Plate Area.....	46
Figure 4-6: Plug to EBF ³ Material on the ND Surface	47
Figure 4-7: Inverse Pole Figure of Each Plate Orientation.....	49
Figure 4-8: Mechanical Properties vs Degrees to DD	50
Figure 4-9: True Strain vs Degrees to DD	51

1 INTRODUCTION

1.1 Background

The growing technology, additive manufacturing (AM), creates complex shapes cheaper, faster, and more customizable than traditional manufacturing technology. AM is defined by ASTM as “a process of joining materials to make objects from 3D model data, usually layer upon layer, as opposed to subtractive manufacturing methodologies” (Alcisto, 2011). The technology started in 1987 with the invention of stereolithography (SL), a primitive process that solidifies layers of ultraviolet (UV) light-sensitive, liquid polymer by exposing it to a laser (Wohlers, 2011). Over the past decades, AM technology has matured and now most techniques incorporate solid freeform fabrication (SFF), which is the production of a freeform, solid object directly from a computer model.

As markets continue to move towards mass customization, more companies are looking at AM to gain a competitive advantage (Da Silveira, 2001). To do this, the limitations and strengths of all aspects of AM technology must be understood. Specifically, how this technology will affect material mechanical properties compared to traditional manufactured material. Understanding this allows companies to judge when and where AM can be used successfully. Continued research must be done on all emerging AM processes to document their mechanical properties.

1.1.1 The EBF³ Process

Electron beam freeform fabrication (EBF³) is an AM and SFF technique that can produce objects directly from a computer-aided design (CAD) model by using a layer-upon-layer technique (Taminger, 2006). EBF³ uses electron beam wire deposition (EBWD) technology, which is a wire feed process that uses an electron beam to create a single bead of material deposited upon subsequent passes until a 3D part is built. EBF³ uses significantly less material than traditional manufacturing processes because it eliminates the need for machining material from wrought blocks or forgings. This process allows for products to be manufactured faster, cheaper, more precise, more intricate, and without consumable tools. EBF³ can also be used to build upon traditional manufacturing processes because it allows material to be directly deposited to specific regions of existing shapes.

A standard EBF³ set-up used for creating linear deposits is depicted in Figure 1-1 (Taminger, 2006). All set-ups require a high-power electron beam gun inside a vacuumed environment. Wire is fed through a spool and into the electron beam which forms a small molten pool. After exposure to the electron beam, the pool rapidly solidifies and a layer of deposit material is created. Layers of this deposit can be built side-by-side, on top of each other, or both.

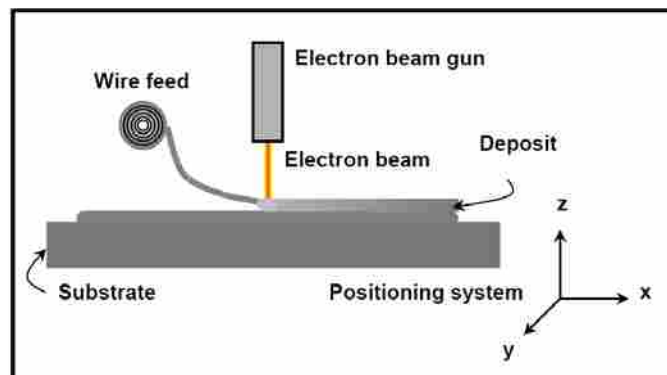


Figure 1-1: Electron Beam Freeform Fabrication System

1.1.2 EBF³ Application to IN 718

Inconel, a nickel-chromium superalloy, is used for a variety of industrial applications including aerospace engineering, oil refinery, nuclear power generation, and food processing. Inconel is corrosion resistant and retains its strength over a wide variation of temperatures making it well-suited for extreme environments of pressure and heat (Paulonis, 2001).

Unfortunately, Inconel is a difficult metal to shape and machine using traditional manufacturing due to rapid work hardening, which is the strengthening of a metal as it undergoes plastic deformation. Inconel requires slow cutting speeds and expensive consumable tools. Furthermore, many Inconel alloys are difficult to weld, but several alloys, including the widely-used Inconel 718 (IN 718), have been developed and optimized for welding applications (Lingenfelter, 1989).

The weldable property of IN 718 makes it a viable material for the EBF³ process. Using EBF³ to process IN 718 allows products to be made faster and cheaper since only post machining is required. Furthermore, using EBF³ can streamline the manufacture of intricate parts because it can be deposited directly to regions where it is needed (Taminger, 2006). However, when IN 718 is processed using EBF³, the mechanical properties are still not fully understood, making specific applications difficult. To utilize the promising future of IN 718 parts processed using EBF³, continued studies must be conducted to fully document the mechanical behavior of this material.

1.1.3 EBF³ Build-up Strategies

Traditionally the EBF³ build-up strategy of IN 718, is a linear stop-go method. This requires creating a layer of deposited material, then allowing it to cool before adding a new layer to the top. Either the wire feed or the support table is moved to control the location of the

deposition layer. Using this technique, large walls and shapes can be built upon the support table or layers can also be deposited onto existing parts. Figure 1-2 depicts a part fabricated using a linear EBF³ build-up strategy (Taminger, 2006).

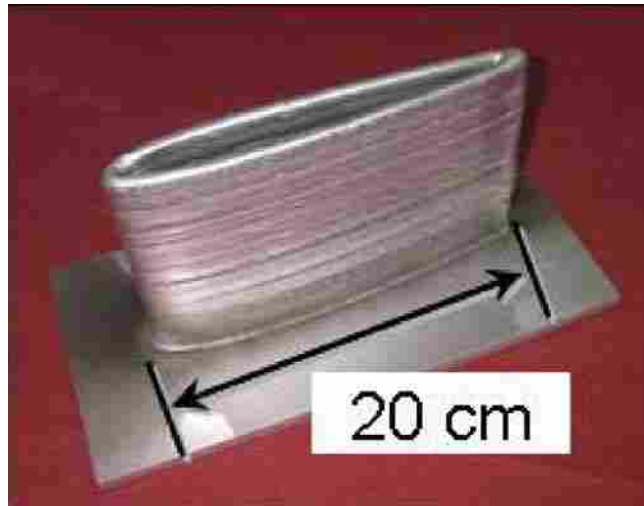


Figure 1-2: IN 718 Fabricated Part Using a Linear EBF³ Build-up

A rotational build-up strategy is a new technique that utilizes a cylindrical shaped part on-which the deposit material is added. This technique does not utilize a support table. The cylinder slowly rotates under the wire feed and electron beam allowing layers to be deposited both side by side and on top of each other without having to stop the process as often as a linear build-up strategy. The mechanical properties of a rotational build-up strategy have yet to be fully documented, limiting the tailored application for this form of EBF³. For the evaluation of the room-temperature, mechanical properties and microstructure of this IN 718 material, a multi-layer thick, plate was created using a rotational build-up strategy. Successive layers were deposited upon each other creating a circular wall with a hot extruded cylinder effectively welded into the center.

Figure 1-3 shows the IN 718 plate that was fabricated for evaluation. The deposition direction (DD), alternatively referred to as the radial direction (RD), depicts the rotational direction of the deposited layers that were built up around the cylinder. The DD surface is labeled as cross-sectional plane. Any cross-sectional plane oriented perpendicular to the DD is referred to as the DD surface. The normal direction (ND) depicts the linear axis through the thickness of the plate. The ND surface is labeled on the top of the plate and is perpendicular to the ND. Any surface plane parallel to the top plate surface is referred to as the ND surface because it will be perpendicular to the ND. The transverse direction (TD) depicts the linear axis through the build-up height of the plate. The TD surface is labeled on the outer surface edge of the plate but any surface plane perpendicular to the TD is referred to as the TD surface.

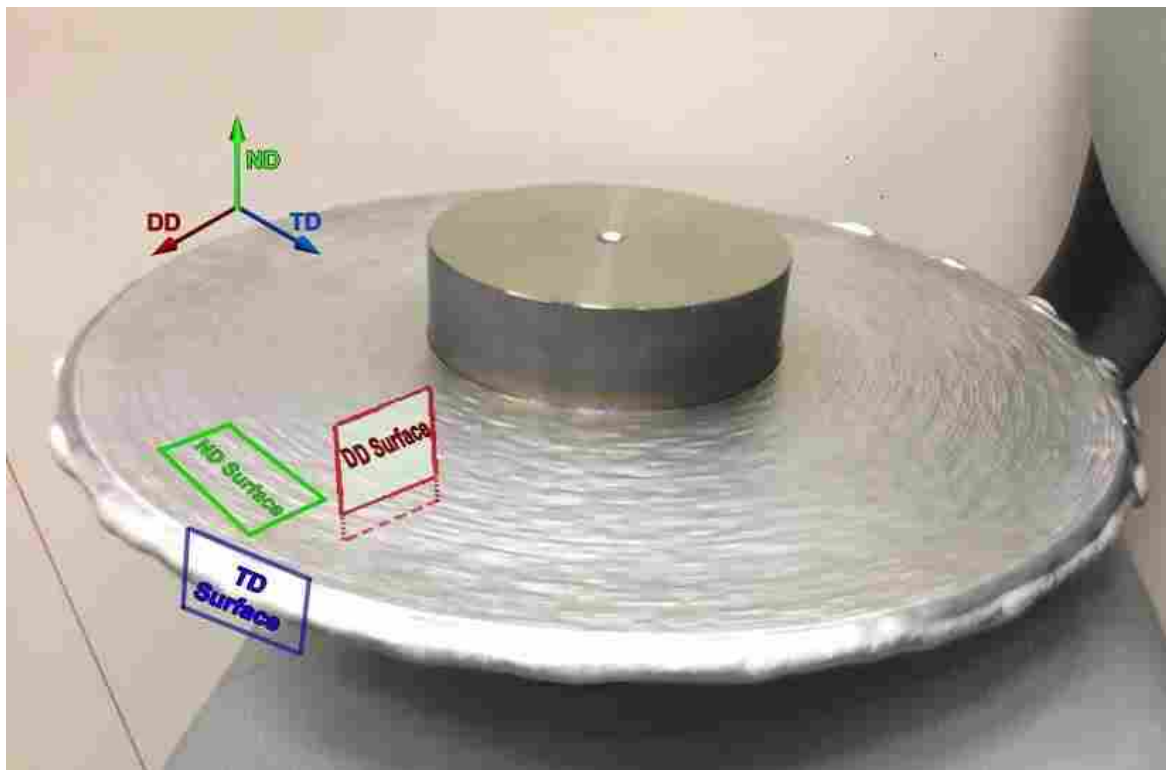


Figure 1-3: Inconel 718 Plate with Respective Orientation Labels

1.2 Hypotheses

H1: Height location vs tensile strength- Yield strength will decrease moving higher along the build height, or TD axis. This hypothesis is based on a concern from the material provider, Lockheed Martin. The concern relates to current literature, which documented an unusual build-up height effect on part strength. Single layer thick parts showed increased strength at higher build-up heights, while multiple layer thick parts showed decreased strength at higher build-up heights (Bird, 2009).

H2: Sample orientation vs tensile strength- The highest yield strength will be in the DD. This hypothesis assumes that the DD will have a high yield strength due to the absence of deposit layer interfaces in this direction. The tensile force will be distributed through-out the length of side-by-side deposited wire rather than pulling through build-up layers.

1.3 Significance of the Study

The material provider, Lockheed Martin, requires understanding of this EBF³ material to potentially utilize it to create a pressure vessel. However, the scope of this study can be defined in broader terms because the processing of IN 718 using EBF³ has the promise to increase manufacturing speed, decrease manufacturing costs, and increase the possible shape complexity of all essential IN 718 items including; gas turbines, safety valves, aircraft engines, etc. This would save millions of dollars annually in manufacturing costs and allows for simpler mass-customization (Taminger, 2008).

This research brings the industry closer to understanding the strengths and limitations of IN 718 processed by EBF³. It will further serve to verify and build upon previous studies of the mechanical properties of IN 718 processed by EBF³. This research will extend the knowledge of

this materials mechanical properties in four ways: 1) it will document the mechanical properties of IN 718 processed using a rotational EBF³ build-up strategy, 2) it will document the mechanical properties at 15 degree increments from 0 to 90 degrees to the DD within the ND Surface, 3) it will document the mechanical properties in the TD, and 4) and it will document the mechanical properties of the transition zone of a mass of IN718 processed by EBF³ attached to a mass of IN 718 processed by extrusion. No past research has fully addressed these variables.

1.4 Delimitations

This study will be performed on IN 718 because of its weldability and wide application across industries. Analysis will only be performed on non-heat treated material. Current literature already documents the benefits of heat treating IN 718 after the EBF³ process (Bird, 2009). This study will only focus on IN 718 processed by EBF³ using a rotational build-up strategy. The rotational build-up strategy is well-suited for creating cylindrical shaped parts and creating additional EBF³ features on traditionally manufactured parts. Other build-up strategies will not be considered for the scope of this research and are documented by previous studies. Lastly, this study will focus on tensile mechanical properties, future studies will need to be conducted to document compression mechanical properties.

1.5 Definition of Abbreviations and Terms

AM- Additive manufacturing; layer upon layer manufacturing technique

ASTM- American Society for Testing Materials; an internationally recognized standard

CAD- Computer-aided design

DD- Deposition direction, can be referred to as RD

DMD- Direct metal deposition or referred to as LENS; AM and SFF technique utilizing LPD

DMLS- Direct metal laser sintering; AM powder bed process utilizing a laser as an energy source

Dogbone- Term given to tensile specimens since they are shaped like a dog bone

E- Modulus; initial slope of stress/strain curve

EBF³- Electron beam freeform fabrication; AM and SFF technique utilizing EBWD

EBSD- Electron backscatter diffraction; type of microscopy

EBWD- Electron beam wire deposition; AM wire feed process utilizing an electron beam as an energy source

EDM- Electrical discharge machine / machining; commonly used to create dogbones

FCC- Face-centered cubic; crystal system where the unit cell is in the shape of a cube

GMAW- Gas arc metal welding; AM wire feed process utilizing a plasma arc as an energy source

Interim dogbone- Used by this study to label a dogbone which crosses a stop-start ring

HT- Heat treatment; heating process conducted on materials to increase strength

IN718- Inconel 718, N07718, Alloy 718; type of nickel-chromium super-alloy

LENS- Laser engineered net shaping or referred to as DMD; AM and SFF technique utilizing LPD

LPD- Laser powder deposition; AM powder injection process utilizing a laser as an energy source

NASA- National Aeronautics and Space Administration

ND- Normal direction

RD- Radial direction, can be referred to as the DD

SEM- Scanning electron microscope; type of microscopy

SFF- Solid freeform fabrication; CAD driven AM technique

SLS- Selective laser sintering- AM and SFF technique utilizing DMLS

SMD- Shaped metal deposition; AM and SFF technique utilizing GMAW

Stop-start ring- Used by this study to define an area where the EBF³ process is stopped and restarted again.

TD- Transverse direction

UTS- Ultimate tensile stress; highest recorded stress before failure

YS- Yield Strength; commonly calculated using a 0.2% offset

2 LITERATURE REVIEW

2.1 Mechanical Properties of Traditional Manufactured IN 718

Traditional manufacturing offers benefits over emerging technology because the process is well-documented and understood. The primary methods used for traditional manufacturing of IN 718 are cast and wrought shaping processes. Table 2-1 refers to typical tensile properties of heat-treated cast IN 718 (U.S. Department of Defense, 1999). It also shows the typical properties of heat-treated wrought IN 718 in the rolling direction (Ruff, 1986).

Table 2-1: Tensile Properties of IN 718 with Respect to Orientation

MFG Process	UTS (MPa)	YS (MPa)	E (GPa)	True Strain (%)
Typical Cast Ref. Data	786	488	---	22.0
Typical Wrought Ref. Data	1376	1186	205	19

2.2 Mechanical Properties of AM Processes of IN 718

As AM continues to mature, multiple processes have been developed to create intricate parts. AM systems are categorized based of their feed stock material and energy sources. Possible feed stock materials are power bed, powder injection, or wire feed. Possible power sources are laser beam, electron beam, or plasma arc. Any AM process can utilize anyone of these combinations to create a part (Frazier, W. E. 2014). The main CAD driven, or SFF, AM

technologies used for IN 718 are: laser engineered net shaping (LENS) or direct metal deposition (DMD), selective laser sintering (SLS), shaped metal deposition (SMD), and electron beam freeform fabrication (EBF³) (Ruan, 2006).

LENS/DMD, utilizes laser powder deposition (LPD) technology by injecting IN 718 powder through nozzles into molten pools created by a focused laser beam. The part is created layer by layer in a shape that is dictated by a CAD model. LENS/DMD has a moderate build rate which can create parts from 1-4 in³/hr with moderate precision (Ruan, 2006).

SLS utilizes direct metal laser sintering (DMLS) technology by tracing a focused laser beam over a tightly compact IN 718 powder bed. The part is created layer by layer in a shape that is dictated by a CAD model. SLS has a slow build rate which can create parts at about 0.3 in³/hr, but it has high precision and can be used to create thin walls (Ruan, 2006). Any laser driven process has a low energy efficiency at 5-10% while an electron beam is 95% energy efficient (Taminger, 2008).

SMD utilizes gas metal arc welding (GMAW) technology which uses a tungsten inert gas (TIG) welding torch as its energy source (Baufeld, 2012). SMD is a similar process to EBF³ because it also uses wire for the feed stock material and parts manufactured using SMD are visually the same as those made by EBF³. SMD has a fast build rate that is slightly slower than EBF³. EBF³ has the fastest build rate and can reach speeds of up to 80 in³/hr. For both processes, the precision is limited by the diameter of the feed wire (Ruan, 2006).

Table 2-2 shows a side by side comparison of the resultant tensile mechanical properties of IN 718 pulled at 1200 degrees Fahrenheit and processed using LENS/DMD (LPD technology), SLS (DMLS technology), and SMD (GMAW technology) (Benn, 2010). The

properties of EBF³ will be reviewed and compared in following sections. All AM processes reviewed are superior to the cast IN 718 but are inferior to wrought IN 718 as previously reference in Table 2-1. SMD produces the most favorable tensile properties.

Table 2-2: Comparison of AM of IN 718

AM Process	UTS (MPa)	YS (MPa)	True Strain (%)
Typical LENS/DMD	1000	650	17
Typical SLS	1103	896	18
Typical SMD	1034	896	25

2.3 Electron Beam Welding Parameters

The majority of EBF³ is performed on modified electron beam welding machinery. All electron beam welding parameters required for favorable IN 718 welds must be maintained to successful perform EBF³ on IN 718. Table 2-3 shows the typical welding parameters required for IN 718 (Ram, 2005).

Table 2-3: Typical Welding Parameters for IN 718

Parameters	Settings
Current	20 mA
Voltage	60 kV
Speed	8 mm s ⁻¹
Gun-work distance	284 mm
Vacuum	10 ⁻⁴ mbar
Heat Input	150 J mm ⁻¹

2.4 Mechanical Properties of IN 718 Processed by EBF³

A detailed review of each EBF³ technique and the parameter settings during manufacturing is necessary to fully understand resulting properties of IN718. Only a linear build-up strategy will be reviewed since a rotational build-up strategy has not previously been studied. All parts reviewed were created using typical welding parameters previously reviewed on Table 2-3.

To understand the typical mechanical properties of IN 718 processed using EBF³, Table 2-4 is a combination of data from Table 2-1 and Table 2-2 with additional data on the mechanical properties of typical IN 718 processed using EBF³ (Bird, 2009). All data is representative of tensile tests performed in the DD and have undergone heat treatment or alternatively were pulled at 1200 degrees Fahrenheit. IN 718 processed by EBF³ shows mechanical characteristics more favorable than cast but less than wrought. It is also superior in strength compared to all other AM, SFF methods.

Table 2-4: Comparison of Manufacturing Processes of IN 718

MFG Process	UTS (MPa)	YS (MPa)	E (GPa)	True Strain (%)
Typical LENS/DMD	1000	650	---	17
Typical SLS	1103	896	---	18
Typical SMD	1034	896	---	25
Typical Cast	786	488	---	19
Typical Wrought	1376	1186	205	19
Typical EBF ³ HT1 Avg.	1242	947	166	22

Although typical mechanical properties have been identified, there is still a high variation of mechanical properties for each individual part created using EBF³. When building IN 718 parts using EBF³, the build parameters to consider are wire diameter, deposition rate, amount of overlap between each bead, and the cooling frequency and duration before adding additional layers. When evaluating a part's test samples' mechanical properties, further parameters must be considered including: the removal location in reference to part height, also referred to as TD location, and the tensile pull orientation of the sample (DD, ND, TD, or any degree rotation in between). Furthermore, heat treatment or solution treatment of the samples will strengthen the mechanical properties.

2.4.1 Part Build Parameters

Build parameters are settings that do not define the physical dimensions of the part, but rather refer to the process and materials originally used to create the part. These parameters are a factor which determines the mechanical properties of each sample removed from a part. Averages are used while comparing mechanical properties of part build parameters to negate the individual sample parameter differences.

As previously discussed, the parameters explored during a part build are: wire diameter, deposition rate, amount of overlap between each bead, and the cooling frequency and duration before adding additional layers. These parameters are controlled with a typical welding machine altered to use the EBF³ process to create parts. This EBF³ machine is shown in Figure 2-1 (Bird, 2010).

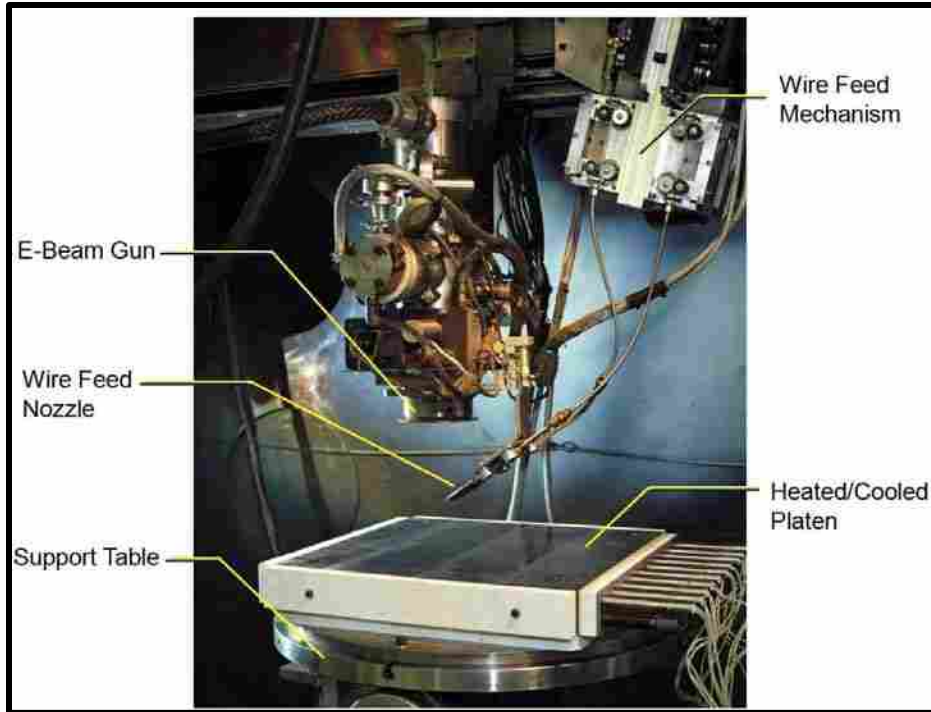


Figure 2-1: A Typical EBF³ Set-up Used on IN 718

To accurately compare IN 718 parts built using EBF³ and their build parameters, a standard definition of part height, width, and length must be created. Table 2-5 shows how this study will define these dimensions for all referenced parts. This is required for accurate comparison of build properties and the literature definitions of these vectors were redefined for this study.

Table 2-5: Height, Width, Length Definitions

	Height	Width	Length
Definition	Created by build layers (on top of each other)	Created by side by side layers	Created by length of deposition bead
Vector Ref.	Z or S	Y or T	X or L
Fabrication Ref. or Orientation	Transverse Direction (TD)	Normal Direction (ND)	Deposition Direction (DD)

To compare build parameters, four parts will be reviewed, which were created and studied by the National Aeronautics and Space Administration (NASA). NASA Wall 1 and NASA wall 2 are shown in Figure 2-2 (Bird, 2009). NASA Block 1 is shown in Figure 2-3 (Bird, 2009). NASA Block 2 is shown in Figure 2-4 (Bird, 2010).

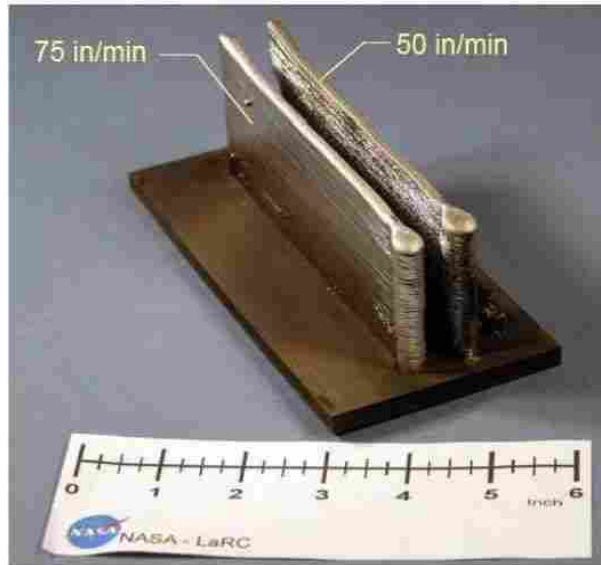


Figure 2-2: NASA Wall 1 (Left) and NASA Wall 2 (Right)

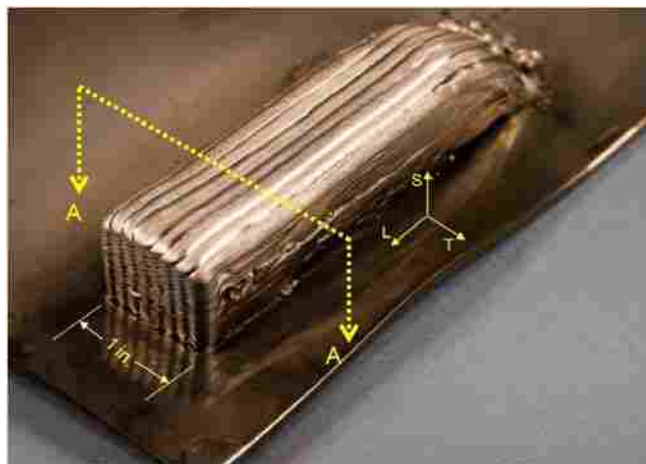


Figure 2-3: NASA Block 1

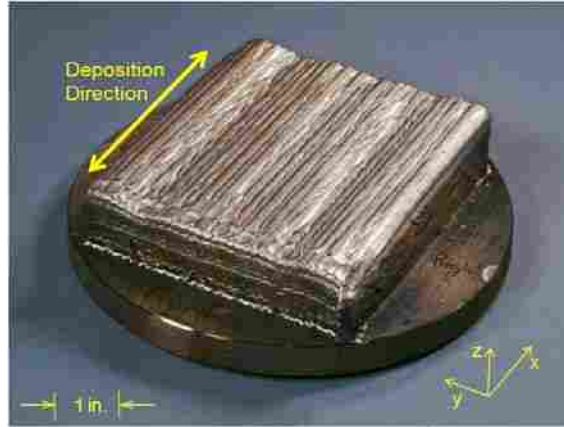


Figure 2-4: NASA Block 2

The respective dimensions and approximate number of layers present in each part build are shown in Table 2-6. Data for NASA Wall 1, NASA Wall 2, NASA Block 1 is shown (Bird, 2009). NASA Block 2 data is also shown (Bird, 2010). The number of layers present in the length is not applicable since this is created by the deposition bead length as previously defined by Table 2-5.

Table 2-6: HxWxL of Each NASA Part

Part	Height (In)	Width (In)	Length (In)	Height (# layers)	Width (# layers)
NASA Wall 1	2	0.125	5	50	1
NASA Wall 2	2	0.125	5	50	1
NASA Block 1	1	1	5	18	8
NASA Block 2	1.1	4.1	4.6	40	34

Table 2-7 refers to the mechanical properties present under set variations of each part build parameter. Data for NASA Wall 1, NASA Wall 2, NASA Block 1 is shown (Bird, 2009). NASA Block 2 data is also shown (Bird, 2010). These results are averages of multiple samples tested from each part. All recorded averages were from samples without post processing such as heat treatment. All samples were pulled in the DD.

Table 2-7: Mechanical Properties of Build Parameters

Part	Wire Dia. (In)	Rate (In/Min)	Deposit Overlap (In)	Cooling Freq. (After "x" Layers)	Cooling Time (min)	UTS (MPa)	YS (MPa)	E (GPa)	True Strain (%)
NASA Wall 1 (Avg.)	0.045	50	N/A	4	2	916	580	160	21
NASA Wall 2 (Avg.)	0.045	75	N/A	4	2	917	584	157	21
NASA Block 1 (Avg.)	0.093	---	0.030	1	1	1022	666	163	23
NASA Block 2 (Avg.)	0.045	---	0.025	1	1.5	978	655	138	27

The feed rate's influence on the mechanical properties is negligible (Bird, 2009). There is evidence that a greater wire diameter plays a role in strengthening mechanical properties but further study is needed to confirm this. All builds required deposit overlap which were targeted at approximate 0.030 inches to avoid the formation of internal voids (Bird, 2009). However, the role of deposit overlap in determining mechanic characteristics is inconclusive. Since different cooling times were used for wall and block parts, the influence of cooling frequency and duration is also inconclusive. For the wall builds, a two minute cooling time was conducted after every 4 layers were added. For the block builds a one minute cooling time was conducted after each layer was added.

2.4.2 Test Sample Parameters

Comparing mechanical properties of test sample parameters also requires averages to negate repetitive data. As a clarification, test sample parameters are physical characteristics of a sample that are a result of how and where a sample was removed from a part. As previously

mentioned, the parameters explored are: the removal location in reference to part height (TD location) and the tensile pull orientation of the sample (DD, ND, TD, or any degree rotation in between). Other sample parameters to consider are the number of deposition layers thick (width) and the number of deposition layers high (height) that are present in the sample. However, as long as the surface area perpendicular to the pull direction captures a significant amount of material grains, the effect of these parameters is negligible.

Table 2-8 shows the dimensions of the samples prepared from each part. Data for NASA Wall 1, NASA Wall 2, NASA Block 1 is shown (Bird, 2009). NASA Block 2 data is also shown (Bird, 2010). The approximate number of deposition layers present in each sample is also recorded. Whenever possible, the ASTM E8 standard dog bone was used as depicted in Figure 2-5 (ASTM, 2001). The sample prepared from NASA block 2 used for TD testing was created through the part’s thickness and therefore required custom dimensions. These dimensions in inches are: 0.450 high, 0.100 wide, and 1.10 long (Bird, 2010).

Table 2-8: Sample Dimensions from Each NASA Part

Part Samples’ dogbones	Height (In)	Width (In)	Length (In)	Height (Layers)	Width (Layers)
NASA Wall 1	0.250	0.125	4.10	6.3	1
NASA Wall 2	0.250	0.125	4.10	6.3	1
NASA Block 1	0.250	0.1	4.10	4.5	0.67
NASA Block 2 (excluding TD)	0.250	0.1	4.10	9.0	0.8

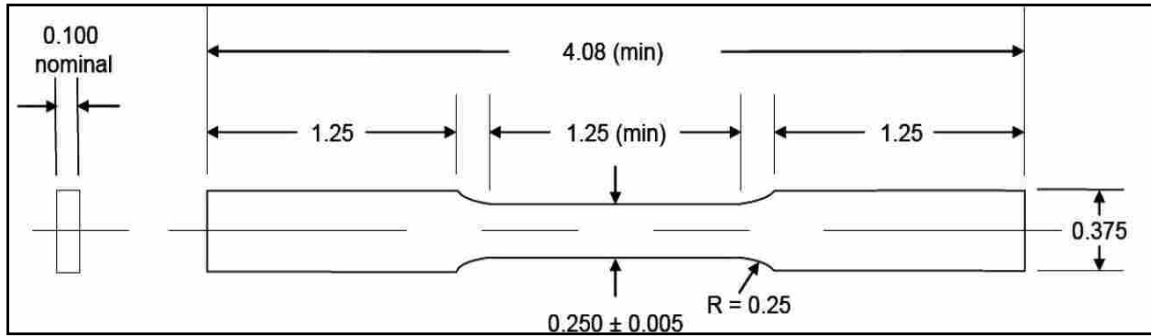


Figure 2-5: ASTM E8 Standard for Subsize Tensile Specimen (in)

Table 2-9 shows the mechanical properties present under different sample parameter variations. Data for NASA Wall 1, NASA Wall 2, NASA Block 1 is shown (Bird, 2009). NASA Block 2 data is also shown (Bird, 2010). As previously stated, these results are averages of duplicate samples tested from each part. All recorded averages were from samples without post processing such as heat treatment.

Table 2-9: Mechanical Properties of Sample Parameters

Smpl. Loc. On Part Height (TD)	Pull Orient.	Rot. (Deg)	UTS (MPa)	YS (MPa)	E (GPa)	True Strain (%)
NASA Wall 1- Bottom (Avg.)	DD	0	897	580	165	21
NASA Wall 1- Top(Avg.)	DD	0	934	581	155	20
NASA Wall 2- Bottom (Avg.)	DD	0	884	542	152	27
NASA Wall 2- Top (Avg.)	DD	0	950	625	163	14
NASA Block 1- Bottom (Avg.)	DD	0	1055	718	168	19
NASA Block 1- Top (Avg.)	DD	0	988	613	159	27
NASA Block 2- Bottom (Avg.)	DD	0	1023	714	139	26
NASA Block 2- Top (Avg.)	DD	0	933	596	136	29
NASA Block 2- Bottom (Avg.)	DD/ND	45/45	1029	789	213	11
NASA Block 2- Top (Avg.)	DD/ND	45/45	958	617	201	23
NASA Block 2- Bottom (Avg.)	ND	0	954	774	195	8
NASA Block 2- Top (Avg.)	ND	0	918	625	192	19
NASA Block 2- N.A. (Avg.)	TD	0	---	---	185	---

The location of the sample in reference to part height, or the TD, shows increased mechanical strength and ductility in samples that were taken from the top of part walls. However, this is reversed in part blocks because samples tested from the bottom of the block

displayed greater mechanical strength and ductility than ones taken from the top (Bird, 2009). This phenomenon is not yet fully understood and requires further study.

The pull orientation plays a significant role in the mechanical properties of the material. The DD properties are most documented and the DD samples demonstrated a reasonably high yield strength but lower modulus values. Samples at 45 degree angles to both the DD and ND (DD/ND), displayed the highest yield strength. For the TD, only the modulus was recorded but it also suggests favorable strength characteristics when compared to the DD. True strain or ductility is also conclusively affected by the orientation direction and had the highest values in the DD (Bird, 2010).

2.4.3 Chemical Composition

The chemical composition is used to ensure none of the parts are volatilized during the build (Bird, 2009). Table 2-10 shows the recorded chemical composition present in each build and stock wire. Data for NASA Wall 1, NASA Wall 2, NASA Block 1 is shown (Bird, 2009). NASA Block 2 data is also shown (Bird, 2010). The nominal chemical composition is also shown for comparison (Brown, 1979).

Table 2-10: Chemical Composition of Each Build, Wire and Nominal

Composition (Wt. %)						
Element	Nominal	0.045 in wire	NASA Wall 1 & 2	0.093 in wire	NASA Block 1	NASA Block 2
Ni	bal.	53.4	53.4	54.08	52.8	54
Cr	19	18.9	18	18.02	18.5	18.1
Fe	18	17.7	17.8	17.93	18.3	17.5
Mo	3	3.1	3.2	3.17	3.07	3.2
Nb	---	5.1	5.7	4.93	5.12	5.3
Ta	---	0	0	0.002	0.002	0
Nb+Ta	5.1	5.1	5.7	4.93	5.12	5.2
Ti	0.9	0.9	1.1	0.89	1.06	1
Al	0.5	0.6	0.6	0.45	0.52	0.5

2.4.4 Microstructure

Figure 2-6 shows the typical dendritic structure observed on the NASA Wall 2 ND surface (Bird, 2009). The layer upon layer build required to perform EBF³ was apparent in the microstructure of the parts. Dendritic structures formed due to the rapid solidification of melted pools. These dendritic structures sometimes stretched across multiple deposition layers and smaller dendritic colonies also formed around each deposition layer. These dendritic structures sometimes stretched across multiple deposition layers and smaller dendritic colonies also formed around each deposition layer.

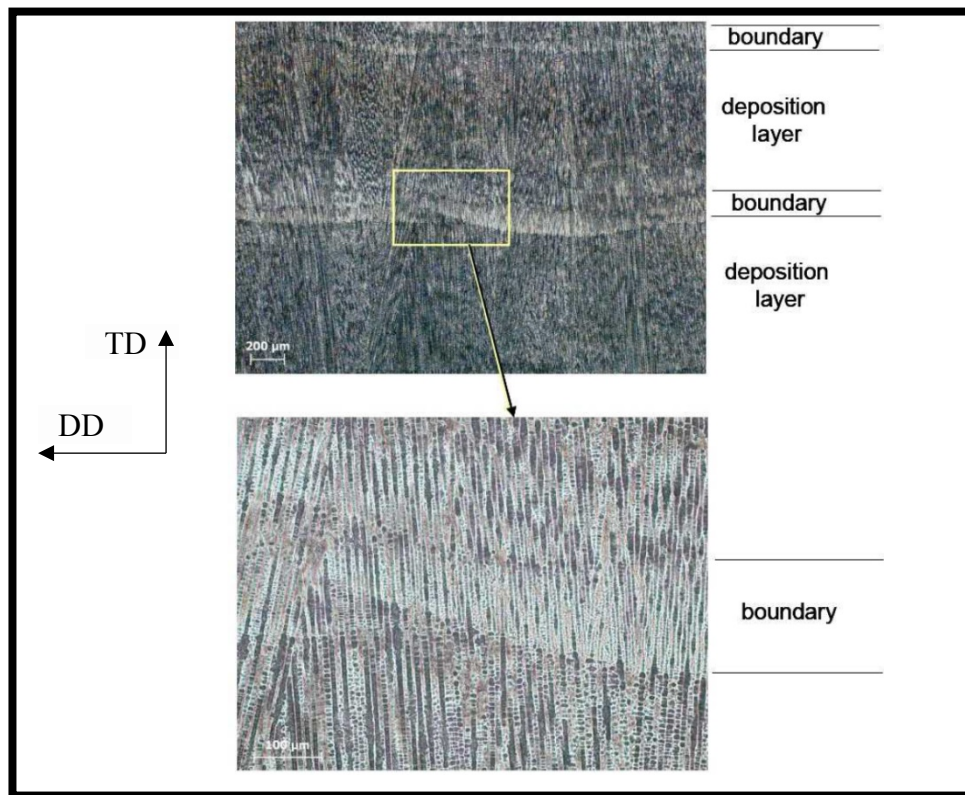


Figure 2-6: Typical EBF³ Dendritic Structure on NASA Wall 2

Figure 2-7 shows the ND surface of NASA Block 2 and also highlights the layered nature of the microstructure along the DD (Bird, 2010). The dendritic structures located low on the part height, or TD location, were smaller and grouped according to the deposition layer. Higher on

the part, a significant fraction of the dendritic structures were larger and penetrated multiple deposition layers. (Bird, 2010). Grain size has a measurable effect on mechanical properties and yield strength typically increases with a decrease in grain size (Dieter,1986). Smaller grains at the bottom of NASA Block 2 most likely accounts for the higher yield strength recorded at the bottom of the part (Bird, 2010).

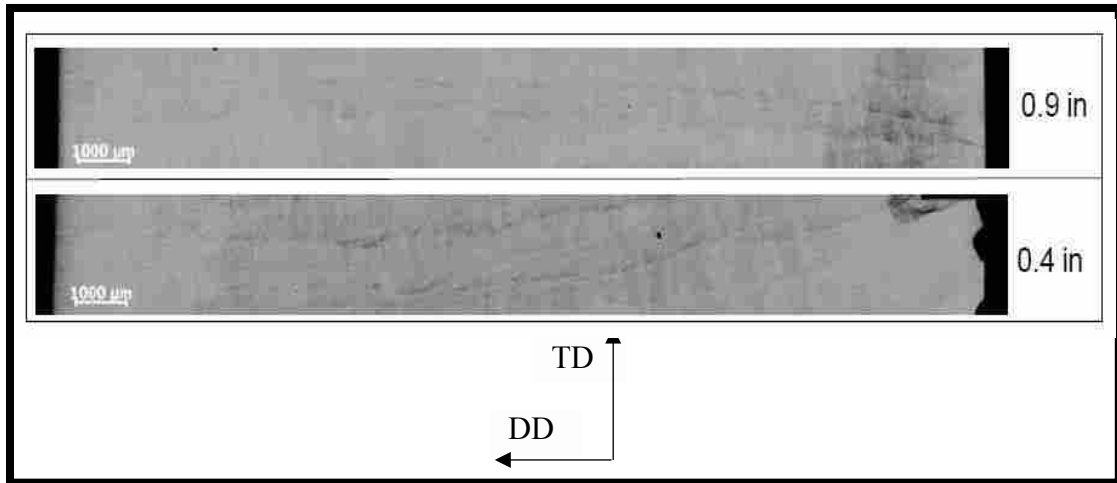


Figure 2-7: NASA Block 2 at 0.4 and 0.9 Inch Build Height

2.4.5 Crystal Orientation

Nickel-base superalloys are composed of face centered cubic (FCC) crystals and their properties are dependent on crystal orientation. The highest ultimate and yield strength are in the $\langle 111 \rangle$ orientation and the greatest ductility is in the $\langle 110 \rangle$ orientation. A low modulus is associated with the $\langle 100 \rangle$ orientation (Dalal, 1984). This is further confirmed as an intrinsic property of nickel as shown in Table 2-11 (Reed, 2008).

Table 2-11: E Value Dependence on Crystal Orientation of Ni

E <111> (Gpa)	E <110> (Gpa)	E <100> (Gpa)
296	220	124

The anisotropy present in the NASA Block 2 material is caused by the strong texture measured in the material. The grains are inhomogeneous and correlate strongly to a set orientation. EBSD scans performed on NASA Block 2 showed a preferential alignment of <011> grains along the TD. A strong <001> texture pattern was also evident along the DD. This data suggests a {011} <100> gross texture within each deposit layer (Tayon, 2014). This texture explains the low E value observed in the DD direction. Further testing is required to fully document the crystal orientation and its influence of the mechanical properties in the DD, TD, and ND.

2.4.6 Heat Treatment

Heat treatment (HT) of IN 718 fabricated by EBF³ provides significant improvements in strength in all orientations. Research has documented the effects of HT under varying parameters. Table 2-12 shows the HT methods performed on samples removed from NASA Block 1 (Bird, 2009). The mechanical properties and microstructure resulting from HT 2 were further documented on samples from NASA Block 2 (Tayon, 2014). The heat treatment serves to solutionize the brittle Laves phase that forms from casting or EBF³ and to homogenize the dendritic microstructure (Handbook, 2005).

Table 2-12: HT Methods Conducted on NASA Block 1

Method	Air Cool to RT (Deg. F & Hrs)	Furnace Cool to 1150 deg. F (Deg. F & Hrs)	Air Cool to RT (Deg. F & Hrs)
HT1 (For Typical Wrought)	1750 for 1 hr	1325 for 8 hrs	1150 for 8 hrs
HT2 (For Typical Casting)	2175 for 4 hrs	1325 for 8 hrs	1150 for 8 hrs

Table 2-13 shows the effect of each HT method and the homogenization of part height properties (Bird, 2009). All samples were pulled in the DD.

Table 2-13: HT Method Effect on Build-up Height Strength

Sample HT method	Loc. On Part Height (TD)	UTS (MPa)	YS (MPa)	E (Gpa)	True Strain (%)
NASA Block 1- HT 1	Bottom	1247	949	168	22
NASA Block 1- HT 1	Top	1238	945	165	21
NASA Block 1- HT 2	Bottom	1123	923	177	20
NASA Block 1- HT 2	Top	1132	942	178	20

The heat treatment helped to create more uniform properties with respect to the part's height or TD. Both methods significantly increased sample strength, but HT 2 resulted in a greater modulus in in the DD. This effect is due to the recrystallization and elimination of deposit layer boundaries (Bird, 2009). HT 2 was more effective at creating recrystallization than HT 1 due to the higher temperature used. The HT 2 microstructure consisted of a bimodal distribution of large and small grains as shown in Figure 2-8 (Bird, 2009)

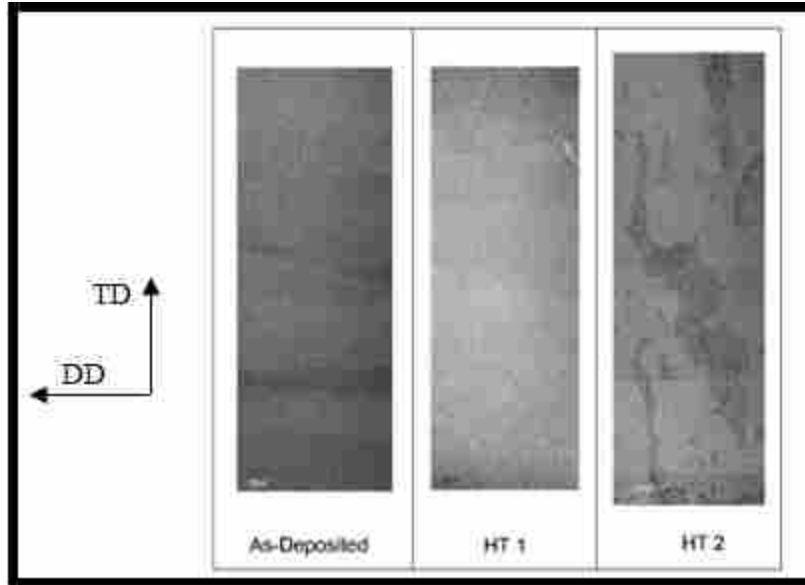


Figure 2-8: Microstructure of As-Deposited and HT

Table 2-14 shows the average mechanical properties recorded after HT 2 with respect to orientation (Tayon, 2014). All orientation directions increased in strength and showed similar strength characteristics besides the DD modulus. However, as previously reviewed, HT 2 still significantly increased DD modulus to closer match the modulus present in other orientations (Bird, 2009).

Table 2-14: HT 2 of IN 718 with Respect to Orientation

Sample HT Method	Pull Orientation	Rot. (Deg)	UTS (MPa)	YS (MPa)	E (Gpa)
NASA Block 2- HT 2	DD	0	1114	986	174
NASA Block 2- HT 2	DD/ND	45/45	1162	998	192
NASA Block 2- HT 2	ND	0	1171	995	193

HT 2 also affects the material's microhardness at each orientation surface as shown in Figure 2-9 (Tayon, 2014). The greatest increase in microhardness was observed on the ND surface. However, the DD/ND surface slightly decreased in hardness.

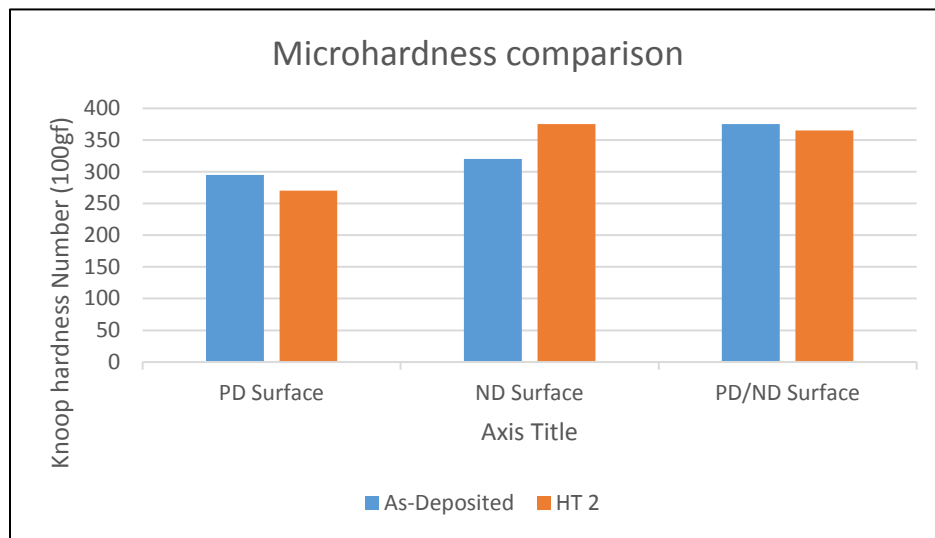


Figure 2-9: Microhardness Evaluation of Crystal Anisotropy

3 METHODOLOGY

3.1 Plate Build Parameters

The EBF³ rotational build-up strategy used to create the IN 718 plate, utilized a 3-inch radius starter plug created by hot extrusion. The starter plug was held horizontally in a lathe type device and deposit was continuously fabricated as the starter plug rotated. The feedstock wire used to create the deposition beads was 0.125 inches in diameter and was made via standard practice by forging rod and drawing it into wire. Each layer was fabricated using standard IN 718 weld parameters by continually depositing 4 beads side by side creating a consistent plate width of approximately 0.5 inches. Deposit beads amount of overlap was not considered for this study.

As the starting plug continuously rotated, new deposition beads were deposited on top of previous layers. Overall, approximately 61 layer rings were laid on top of each other creating a plate 9 inches in radius, including the plug. Each bead laid was approximately 0.225 inches wide and 0.1 inches high excluding overlap. Table 3-1 shows the plate build dimensions; outer circumference could alternatively be defined as length, since all build parameters identified fall within the definitions previously provided by Table 2-5.

Table 3-1: Build Dimensions of IN 718 Plate

Sample	Height (In)	Width (In)	Outer Circumference (In)	Height (# layers)	Width (# layers)
Plate	6.0	0.5	56.5	61	4

The fabrication process was performed as one continuously fed deposition bead until steady state was reached with only two stop-start points occurring. At each stop-start point the continuous deposition bead was ended and restarted again. The first stop-start point occurred after approximately 30 layers, the second after approximately 15 more layers. The duration of the stop or cooling time was not considered for this study. This study focuses on the implications caused by stopping the fabrication process and restarting it again. Figure 3-1 shows where steady state occurred as well as the two stop-start areas.

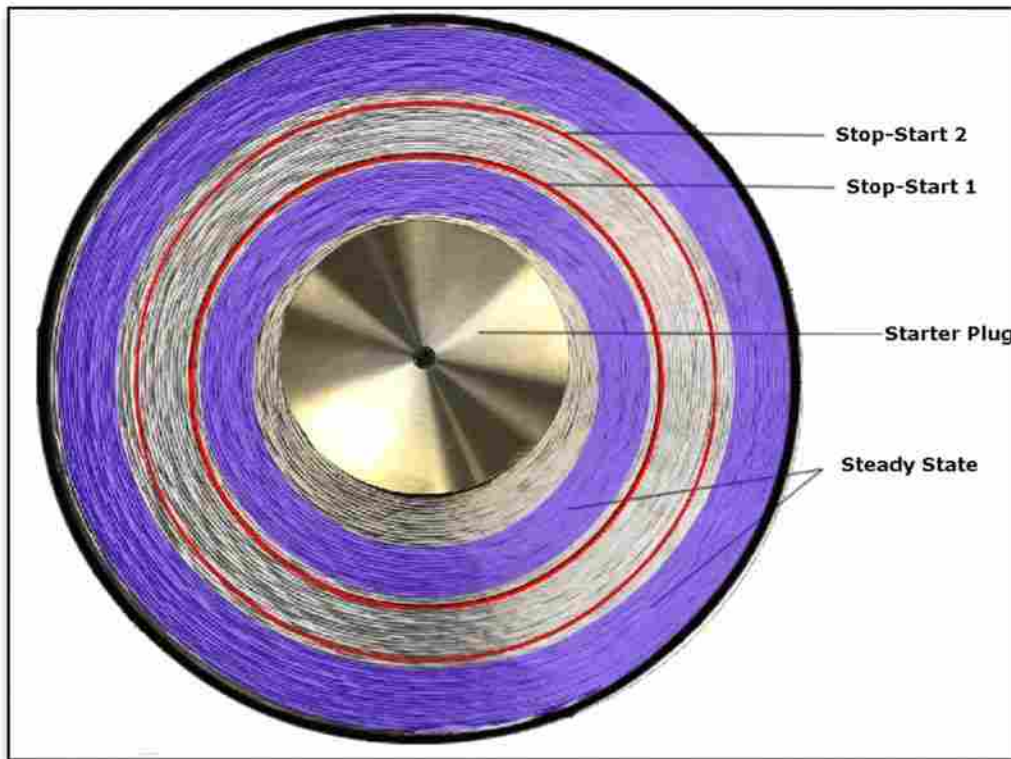


Figure 3-1: IN 718 Plate Fabrication Details

3.2 Test Sample Parameters

Samples were removed from the plate at approximately 15 degree increments starting from 0 degrees to the DD up to 90 degrees to the DD, within the ND surface plane. Figure 3-2 shows each sample's removal region. The areas where microscopy analysis was performed are marked as well.

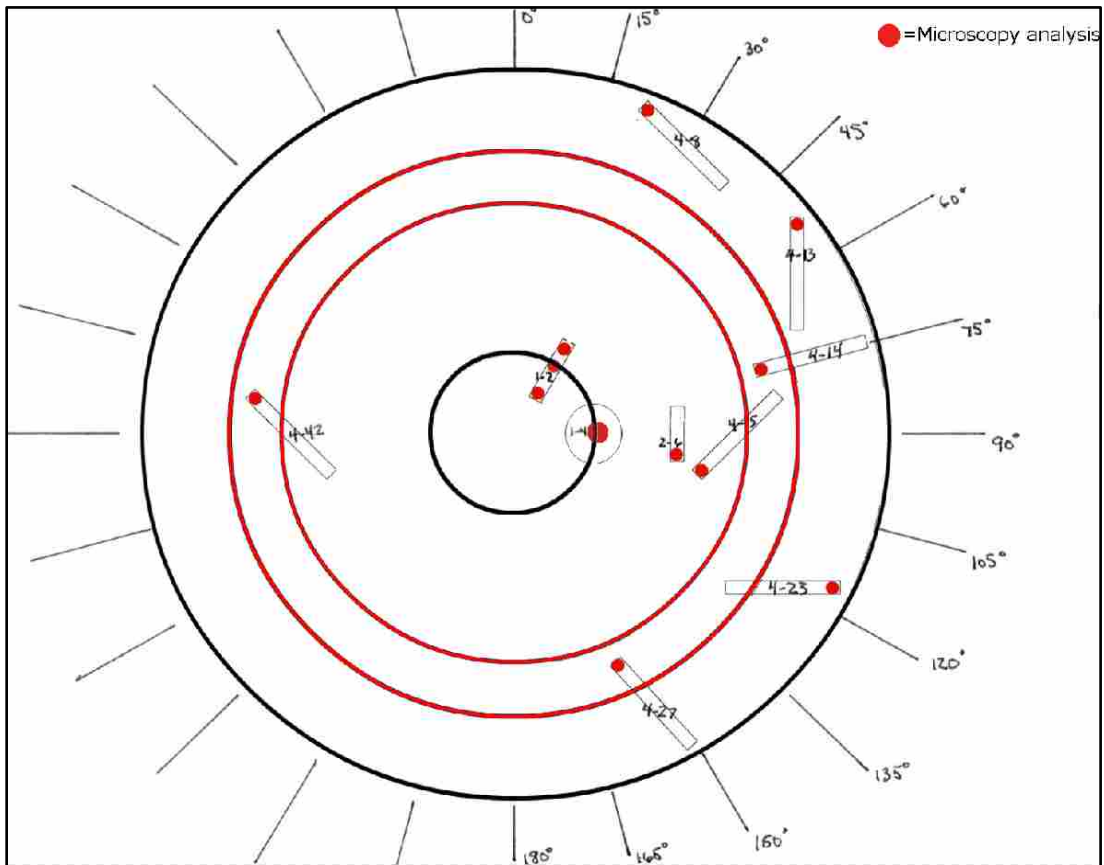


Figure 3-2: Areas of Sample Removal and Microscopy Analysis

Samples removed were generally 4.25 inches in length and 0.5 inches wide, aside from sample 1-4 which was a circle and only used for microscopy. To fully document the material's properties, samples were removed from all regions of the plate. Table 3-2 shows the respective regions and orientations of each sample. No samples oriented in the ND were created.

Table 3-2: Sample Regions and Orientations

Sample	Region	Aprox. Deg. to DD	Closest Orientation
1-2	Plug to EBF3	90	TD
1-4	Plug to EBF3	NA	NA
2-6	Inner Steady State	0	DD
4-8	Outer Steady State	15	DD
4-13	Outer Steady State	30	DD
4-14	Stop-Start 2	90	TD
4-15	Stop-Start 1	45	TD/DD
4-23	Stop-Start 2	60	TD
4-27	Stop-Start 2	75	TD
4-42	Start Stop 1	45	TD/DD

3.2.1 Microscopy Preparation

As previously stated Figure 3-2 identified the specific sample regions where microscopy was performed. All surface orientations of each sample were analyzed. To accomplish this a small portion of the end of each sample was removed as shown in Figure 3-3. The top of the plate references the ND surface and is always parallel to the surface orientation labeled 3. The surface orientation labeled 1 is always perpendicular to the sample pull direction.

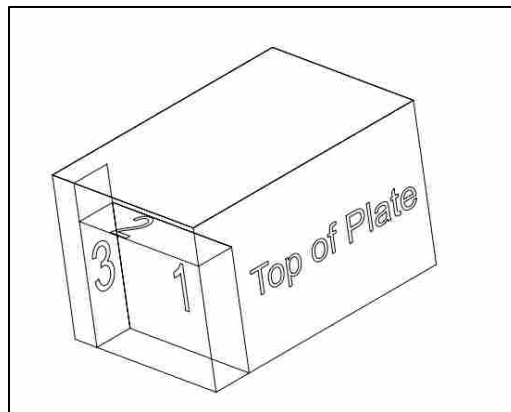


Figure 3-3: Surface Orientations Cut from Each Sample

Surface orientations 1, 2, and 3 were clearly marked with colored clips then set into epoxy pucks as shown in Figure 3-4. Mounting each orientation into an epoxy puck made polishing possible. The puck also attached to a stage to hold samples during microscopy.



Figure 3-4: Sample Orientations Mounted in Puck

The sample pucks were polished for 1 minute on successive grits until they were smooth enough for diamond polishing. The samples were then polished for 3 minutes with 6 micron, 3 micron, and 1 micron diamond paste. To finish, the puck was submerged in a propylene glycol solution and a 30 second electro-polish was performed on each sample within the puck. This preferentially etched the grain boundaries on a microscopic scale producing good contrast images. This was sufficient to perform EBSD microscopy on each sample. For optical microscopy, each sample puck was additionally etched for 30 seconds in a Waterless Kallings etchant.

3.2.2 Tensile Testing

To perform tensile tests, two to four dogbones were prepared from each sample using a wire electrical discharge machine (EDM) with very high precision. Table 3-3 records the dimensions of each tensile sample in inches and the approximate number of deposition layers present. Measures were taken to ensure the surface area of the dogbone perpendicular to the pull direction captured a significant amount of material grains.

Table 3-3: Tensile Test Sample Dimensions

Part Samples' Dogbones	Height (In)	Width (In)	Length (In)	Height (Layers)	Width (Layers)
Plate	0.16	0.079	0.63	0.71	0.79

Figure 3-5 shows the surface of the samples where each dogbone was cut out. As previously discussed, the top of the plate references the ND surface.

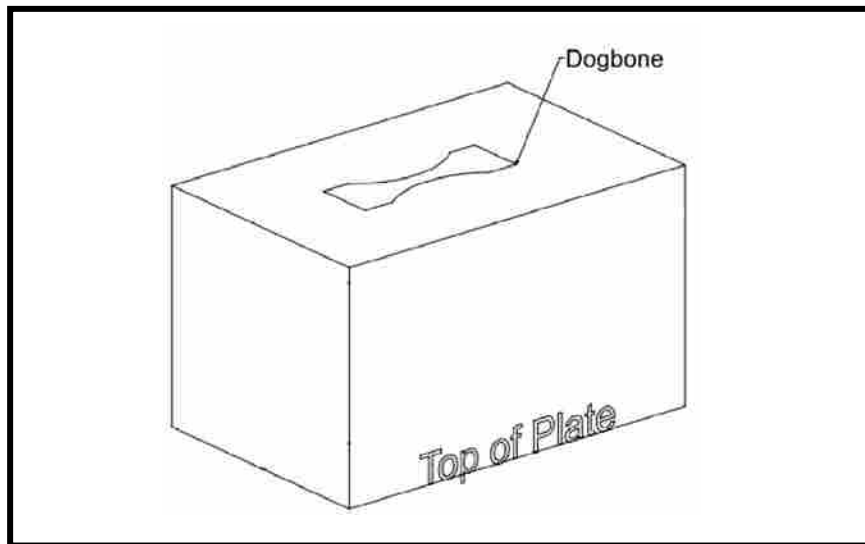


Figure 3-5: Location of Dogbones Cut from Each Sample

Figure 3-6 shows the details of the dogbone size used for tensile testing. This smaller, custom dogbone size was used so it could fit onto the small surface area of the samples. The dogbones were 2 millimeters thick and their total length was 55mm. Samples were pulled at 4 millimeters per minute. The modulus and yield strength were calculated using a 0.2% offset and regression analysis was used to determine the slope (modulus).

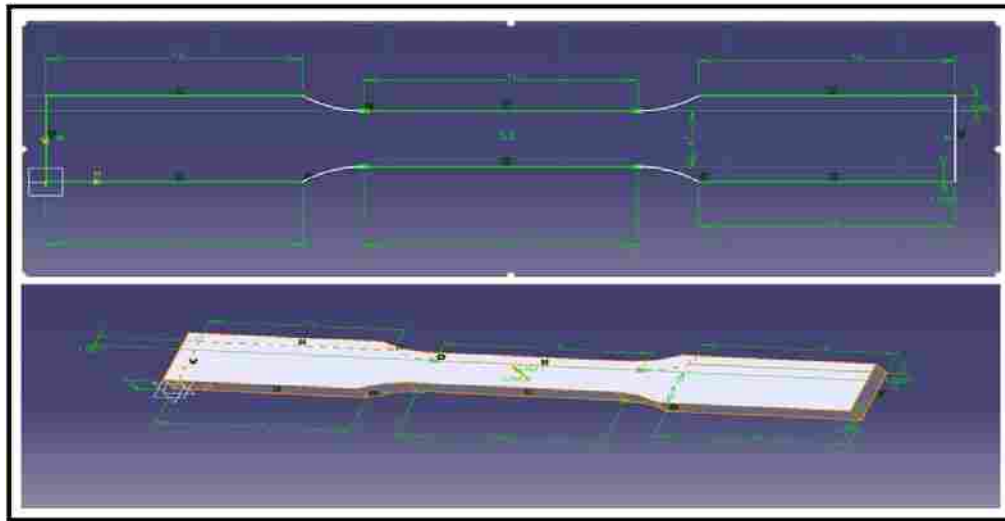


Figure 3-6: Dogbone Dimensions Used for Tensile Testing (mm)

Samples that crossed over stop-start rings, had dogbones created in both the steady state zone and over stop-start rings. This determined if stopping and starting the process causes weak points in the part. For easy reference, dogbones which crossed over a stop-start ring were labeled as interim samples.

3.3 H1: Height Location vs Tensile Strength

As shown in Figure 3-2, samples were selected for tensile testing that represented different areas within the build-up height along the TD axis. Sample 1-2 is located on the inner

part of the plate, which is a low build-up height and Sample 4-8 is on the outer part of the plate, which is a high build-up height. To perform yield strength comparisons, sample orientations must be similar. Samples 2-6 is located on the inner part of the plate and 4-8 is on the outer. These can be used for yield strength comparison since both are oriented in the DD.

3.4 H2: Sample Orientation vs Tensile Strength

As shown in Figure 3-2 samples were selected for tensile testing that represented incremental angles to the DD within the ND surface plane. Sample 2-6 documents tensile testing pulled directly in the DD and Samples 4-14 and 1-2 document mechanical properties perpendicular to the DD. All other samples document the behavior of an incremental degree to the DD within the ND surface plane.

4 RESULTS AND DISCUSSION

4.1 Raw Data Results

Table 4-1 shows the raw data results of all tensile tests performed. As previously discussed, samples that cross a stop-start ring are considered interim. All dogbones from sample 1-2 are considered transitional since they transition from forged plug material to EBF³ material. Table 4-1 also provides a reference of the unique sample parameters of each sample.

Table 4-1: Tensile Test Results

Sample	Region	Approx. Deg. to DD	Closest Orientation	Transitional or Interim	UTS (MPa)	YS (MPa)	E (GPa)	True Strain (%)
1-2	Plug to EBF3	90	TD	Transitional	841	373	145	49
	Plug to EBF3	90	TD	Transitional	840	448	141	45
2-6	Inner Steady State	0	DD	No	917	607	237	38
	Inner Steady State	0	DD	No	912	613	245	31
4-8	Outer Steady State	15	DD	No	813	525	190	31
	Outer Steady State	15	DD	No	834	501	181	32
	Outer Steady State	15	DD	No	785	500	133	31
4-13	Outer Steady State	30	DD	No	970	561	218	28
	Outer Steady State	30	DD	No	978	588	239	30
4-14	Stop-Start 2	90	TD	Interim	779	430	131	32
	Stop-Start 2	90	TD	Interim	736	421	133	31
	Stop-Start 2	90	TD	Interim	797	437	129	26
	Stop-Start 2	90	TD	Interim	775	422	123	34
4-15	Stop-Start 1	45	TD/DD	No	1009	606	256	31
	Stop-Start 1	45	TD/DD	No	1009	603	243	32
	Stop-Start 1	45	TD/DD	Interim	988	596	245	30
	Stop-Start 1	45	TD/DD	Interim	961	551	250	31
4-23	Stop-Start 2	60	TD	No	888	537	185	34
	Stop-Start 2	60	TD	No	879	522	184	34
	Stop-Start 2	60	TD	Interim	903	506	181	30
	Stop-Start 2	60	TD	Interim	889	515	174	30
4-27	Stop-Start 2	75	TD	No	872	490	156	30
	Stop-Start 2	75	TD	No	859	474	169	32
	Stop-Start 2	75	TD	Interim	880	490	153	34
	Stop-Start 2	75	TD	Interim	871	485	156	34
4-42	Stop-Start 1	45	TD/DD	No	930	566	211	38
	Stop-Start 1	45	TD/DD	No	936	647	301	30
	Stop-Start 1	45	TD/DD	Interim	941	588	215	30
	Stop-Start 1	45	TD/DD	Interim	964	565	230	33

4.1.1 Plate Build Parameters

The build parameters, as previously discussed, are settings that do not define the physical dimensions of the part but rather refer to the process and materials originally used to create the part. A focus of the build parameters of the IN 718 plate, was to determine the effect of the stop-start rings on the materials mechanical properties. Table 4-2 shows if dogbone specimens are non-interim or interim, which is defined as crossing over a stop-start ring.

Table 4-2: Interim vs Non-interim and Transitional Properties

	Sample	UTS (MPa)	YS (MPa)	E (GPa)	True Strain (%)
Stop-Start 1	4-15 (Non-interim avg)	1009	605	250	32
	4-15 (Interim avg)	975	574	248	31
	4-42 (Non-interim avg)	933	607	256	34
	4-42 (Interim avg)	953	577	223	32
Stop-Start 2	4-23 (Non-interim avg)	884	530	185	34
	4-23 (Interim avg)	896	511	178	30
	4-27 (Non-interim avg)	866	482	163	31
	4-27 (Interim avg)	876	488	155	34
Plug to EBF ³	1-2 (Transitional avg)	841	411	143	47

By comparing strength test results of non-interim versus interim dogbones, it is apparent that stopping and restarting the process has a negligible effect on the strength properties of the material. This means the EBF³ process can be stopped and started again without compromising overall part strength or creating weak areas where the addition EBF³ build-up is added.

Table 4-2 also shows the average strength properties of sample 1-2 which transitions from the starter plug to EBF³ material and is oriented in the TD. When compared to samples 4-23 and 4-27, which are also oriented in the TD, the results show a slight loss in strength and

significant increase in elongation in sample 1-2. Understanding the loss of strength in this area is crucial to successfully use EBF³ to add material onto existing forged and cast parts.

Since the wire diameter used to create the plate was 0.125 inches, this study can build upon previous studies to document the effect of wire diameter on the materials mechanical properties. Table 4-3 pulls data from Table 2-7 as well as adds in Sample 2-6 data points. Sample 2-6 was chosen because it is oriented in the DD, which is the same orientation used on previous studies (Bird, 2009). Table 4-3 shows that wire diameter is negligible in predetermining the strength of a part fabricated using EBF³.

Table 4-3: Strength vs Wire Diameter

Part	Wire Dia. (In)	UTS (MPa)	YS (MPa)	E (GPa)	True Strain (%)
NASA Block 2 (Avg.)	0.045	978	655	138	31
NASA Block 1 (Avg.)	0.093	1022	666	163	26
Plate Sample 2-6 (Avg.)	0.125	915	610	241	35

4.1.2 Test Sample Parameters

Test sample parameters are physical characteristics of a sample that are a result of how and where a sample was removed from a part. As previously mentioned the parameters explored are: the removal location in reference to part height (TD location) and tensile pull orientation of the sample (DD, ND, TD, or any degree rotation in between). Table 4-4 shows the strength characteristics of each sample averaged across all tensile pulls. Sample 1-2 transitions from the forged plug to the EBF³ material, so it cannot be directly compared to the other samples.

Table 4-4: Mechanical Properties of Plate Test Sample Parameters

Sample	Location on part height (TD)	Aprox. Deg. to DD	Closest Orientation	UTS (MPa)	YS (MPa)	E (GPa)	True Strain (%)
1-2 (avg)	Transitional	90	TD	841	411	143	47
4-15 (avg)	Middle	45	TD/DD	992	589	249	33
4-42 (avg)	Middle	45	TD/DD	943	592	239	33
2-6 (avg)	Inner	0	DD	915	610	241	35
4-8 (avg)	Outer	15	DD	811	509	168	31
4-13 (avg)	Outer	30	DD	974	575	229	29
4-14 (avg)	Outer	90	TD	772	428	129	31
4-23 (avg)	Outer	60	TD	890	520	181	32
4-27 (avg)	Outer	75	TD	871	485	159	33

The mechanical properties of the plate in reference to movement along the TD, or part height, can best be analyzed by looking at the inner versus outer mechanical properties. The most direct comparison can be made by looking at sample 2-6 and 4-8 because they are both oriented in the DD, but one is inner and one is outer. This shows a decrease in both yield and ultimate strength occurs when build-up height increases. This is consistent with previously reviewed studies conducted on block, or multi-layer thick EBF³ material (Bird, 2009).

Regarding orientation, the highest ultimate strength and modulus was in the TD/DD, or 45 degrees to the DD, as recorded by sample 4-15. Sample 2-6 is oriented in the DD and demonstrated the highest yield strength, which was slightly higher than the TD/DD yield strength. The weakest orientation was in the TD, or 90 degrees to the DD, with Sample 4-14 being exactly oriented in the TD and demonstrating the lowest ultimate strength, yield strength and modulus. Previously reviewed studies never conducted tensile tests in the TD but rather tested only the ND and DD (Bird, 2010). Ductility is similar across all orientations, but the DD demonstrated the highest true strain as shown by sample 2-6.

Figure 4-1 shows the stress/strain curve for each sample and is organized by orientation to the DD (within the ND surface plane) and part height. Detailed analysis of the differences in

properties with regards to orientation will be revisited when crystal orientation and texture is examined.

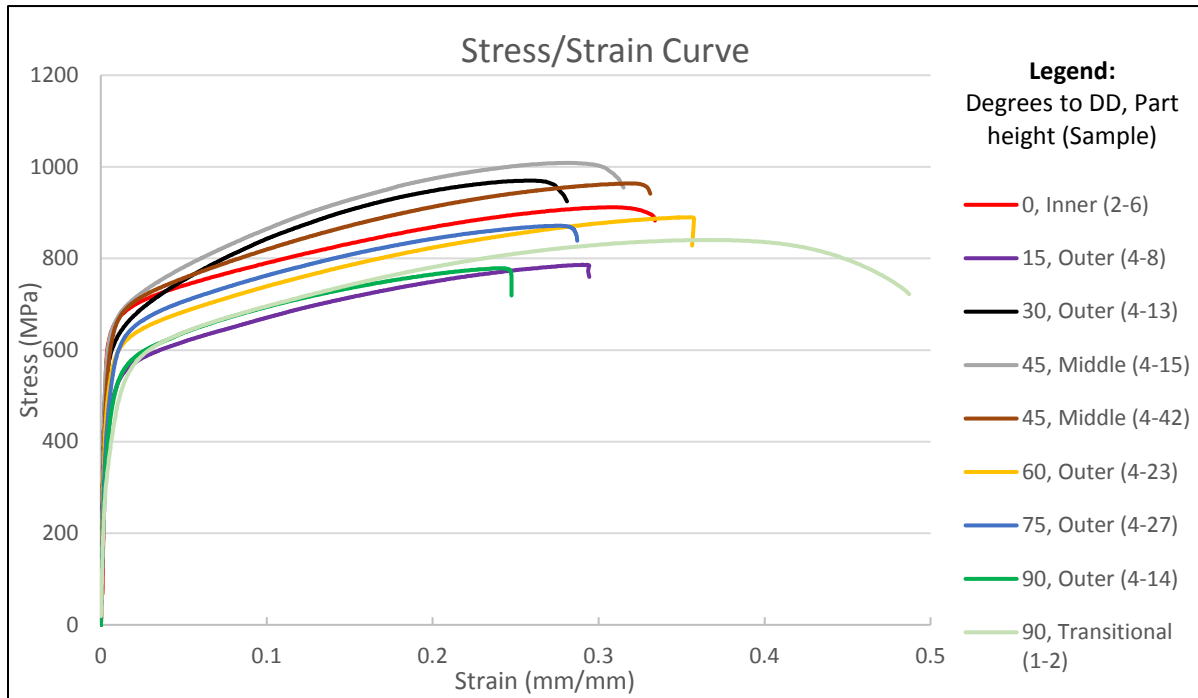


Figure 4-1: Stress/Strain Curve of Each Sample

In previously reviewed studies, the DD/ND demonstrated the highest ultimate strength and was only slightly superior to the DD (Bird, 2010). Since the TD/DD was recorded as the highest ultimate strength for this study, this suggests that any pull orientation 45 degrees to the DD will demonstrate a high ultimate strength for IN 718 manufactured using EBF³.

4.1.3 Chemical Composition

Chemical composition testing was independently performed by Lockheed Martin to ensure the plate was not volatilized during the build. All results fell within the nominal value provided on Table 2-10.

4.1.4 Microstructure

Table 4-5 shows the surface orientation information needed to analyze each sample's microstructure. Through matching surface orientations, overall plate microstructure can be analyzed to better understand the behavior of the material's mechanical properties. Areas of analysis include: dendritic structure and texture with regard to the TD (build-up height), dendritic structure and texture at the plug to the EBF³ transition zone, and IN 718 crystal orientation with regards to the DD, ND and TD.

Table 4-5: Microscopy Labels Matched to Plate Surface Orientations

Sample	Region	Approx. Deg. to DD	Closest Tensile Pull Orientation	Microscopy Label	Closest Surface Orientation
1-2-Plug	Plug	90	TD	1	TD
				2	DD
				3	ND
1-2-EBF ³	Inner (Steady State)	90	TD	1	TD
				2	DD
				3	ND
1-4	Plug to EBF ³ Inner (Steady State)	NA	NA	3	ND
2-6	Inner (Steady State)	0	DD	1	DD
				2	TD
				3	ND
4-8	Outer (Steady State)	15	DD	1	DD
				2	TD
				3	ND
4-13	Outer (Steady State)	30	DD	1	DD
				2	TD
				3	ND
4-14	Outer (Stop-Start 2)	90	TD	1	TD
				2	DD
				3	ND
4-15	Inner (Stop-Start 1)	45	TD/DD	1	TD/DD
				2	TD/DD
				3	ND
4-23	Outer (Stop-Start 2)	60	TD	1	TD
				2	DD
				3	ND
4-27	Outer (Stop-Start 2)	75	TD	1	TD
				2	DD
				3	ND
4-42	Inner (Start Stop 1)	45	TD/DD	1	TD/DD
				2	TD/DD
				3	ND

4.1.4.1 Microstructure Along the TD

Figure 4-2 shows the microstructure grain size and shape at 0 degrees to the DD, 45 degrees to the DD and 90 degrees to the DD within the ND surface plane. All orientation surfaces are to scale within relation to each other and labeled with a 400 micron scale bar. The grain shape and direction corresponded strongly to the TD and stretch across deposition layers rather than along them. Figure 4-3, Figure 4-4, and Figure 4-5 show electron backscatter diffraction (EBSD) scans and optical microscopy imagery for each surface orientation, starting with the inner plate area moving along the TD axis to the middle and outer area. The images can be oriented by sight since Figure 4-2 shows that the long column-shaped grains run from the center of the plate to the outer edge, or in other words along the TD axis.

The TD surface shows grains approximately 0.5-1 millimeters in size. These grains then stretch along the TD, as shown by the DD surface and ND surface images, and are 2-3 millimeters in length. Near the inner areas these grains are predominantly linear. As the microscopy scans move towards the middle area of the plate they show that these linear grains start to widen. Finally, near the outer area the grains there are not as long, but rather they become somewhat less columnar.

As previously discussed, grain size has a measurable effect on mechanical properties, and yield strength typically increases with a decrease in grain size (Dieter, 1986). The section closer to the plug has columnar grains with close spacing between them along the DD direction, resulting in higher yield strength. At the outer section, or high build-up height, the grains are no longer thin columns and spread out creating larger grains which results in a decrease in yield strength.

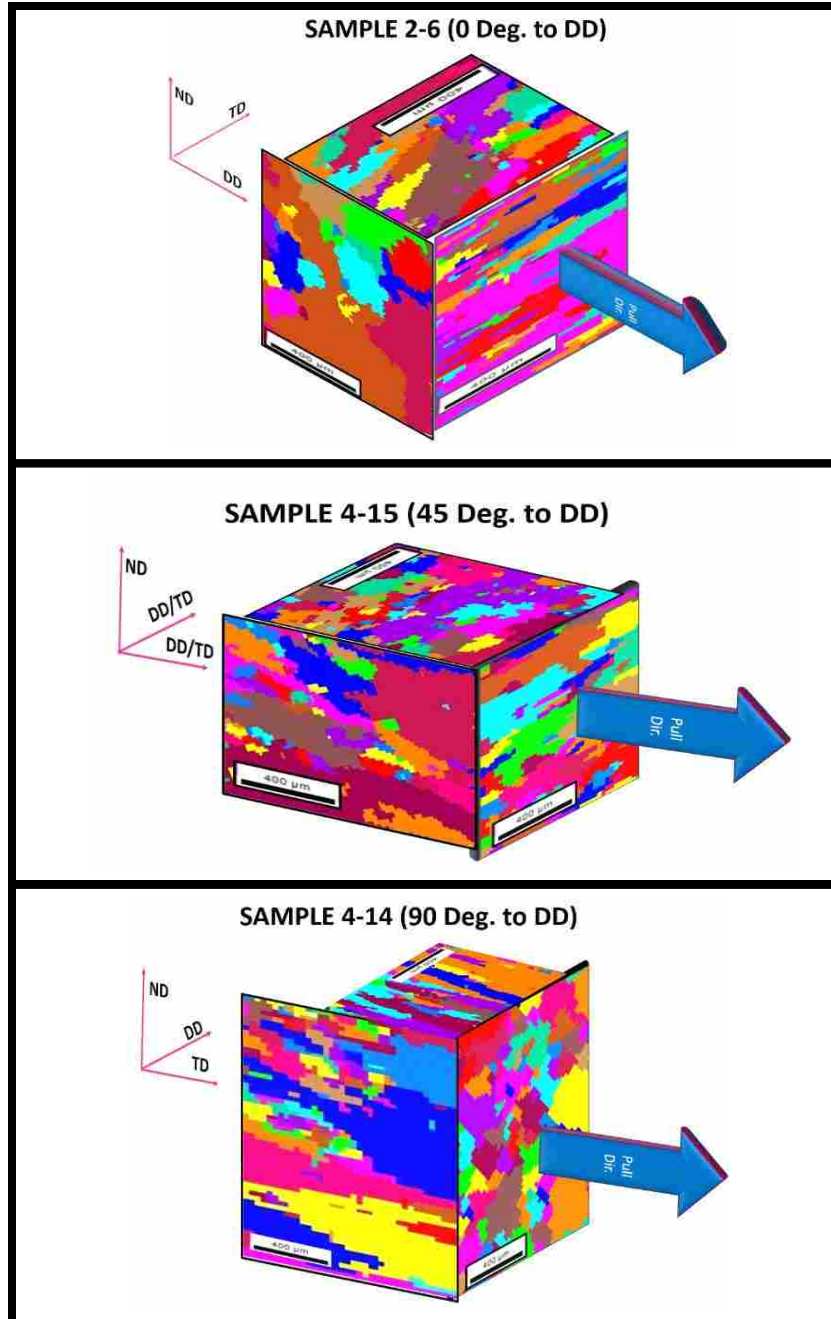


Figure 4-2: Grain Size and Shape at 0, 45, and 90 Degrees to DD

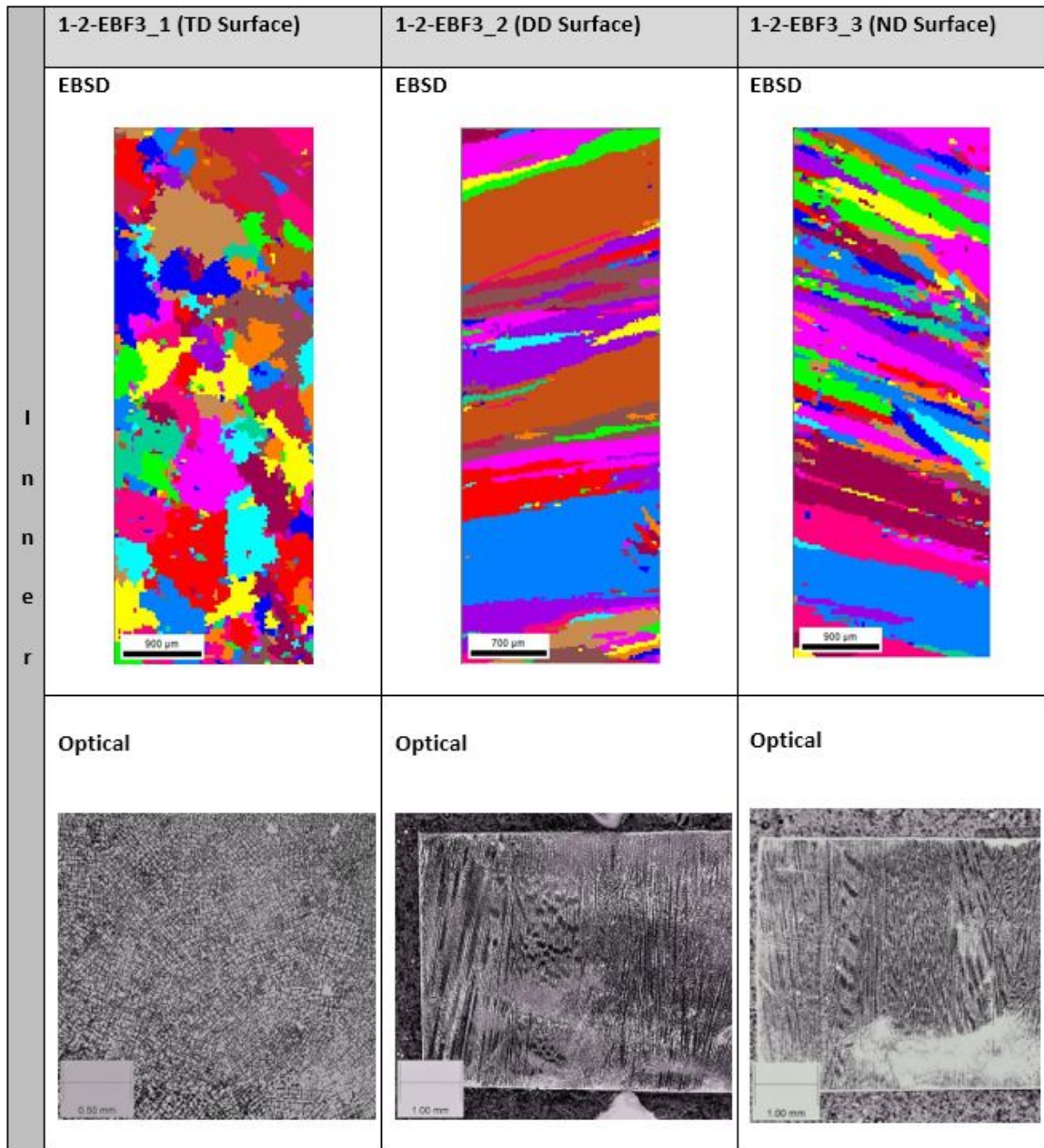


Figure 4-3: Each Surface Orientation at the Inner Plate Area





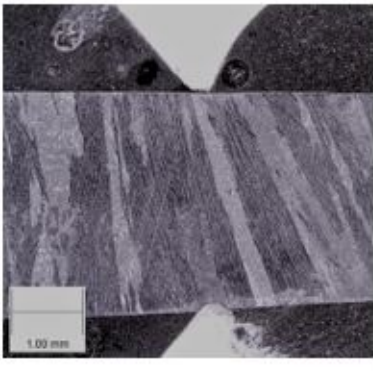
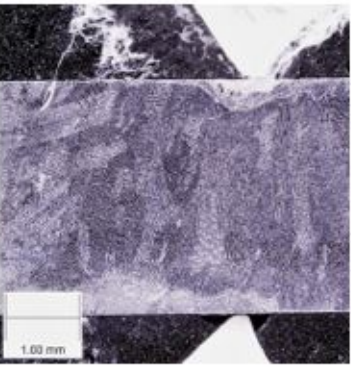
	4-14_1 (TD Surface)	4-14_2 (DD Surface)	4-14_3 (ND Surface)
M i d d l e	EBSD 	EBSD 	EBSD 
	Optical 	Optical 	Optical 

Figure 4-4: Each Surface Orientation at the Middle Plate Area

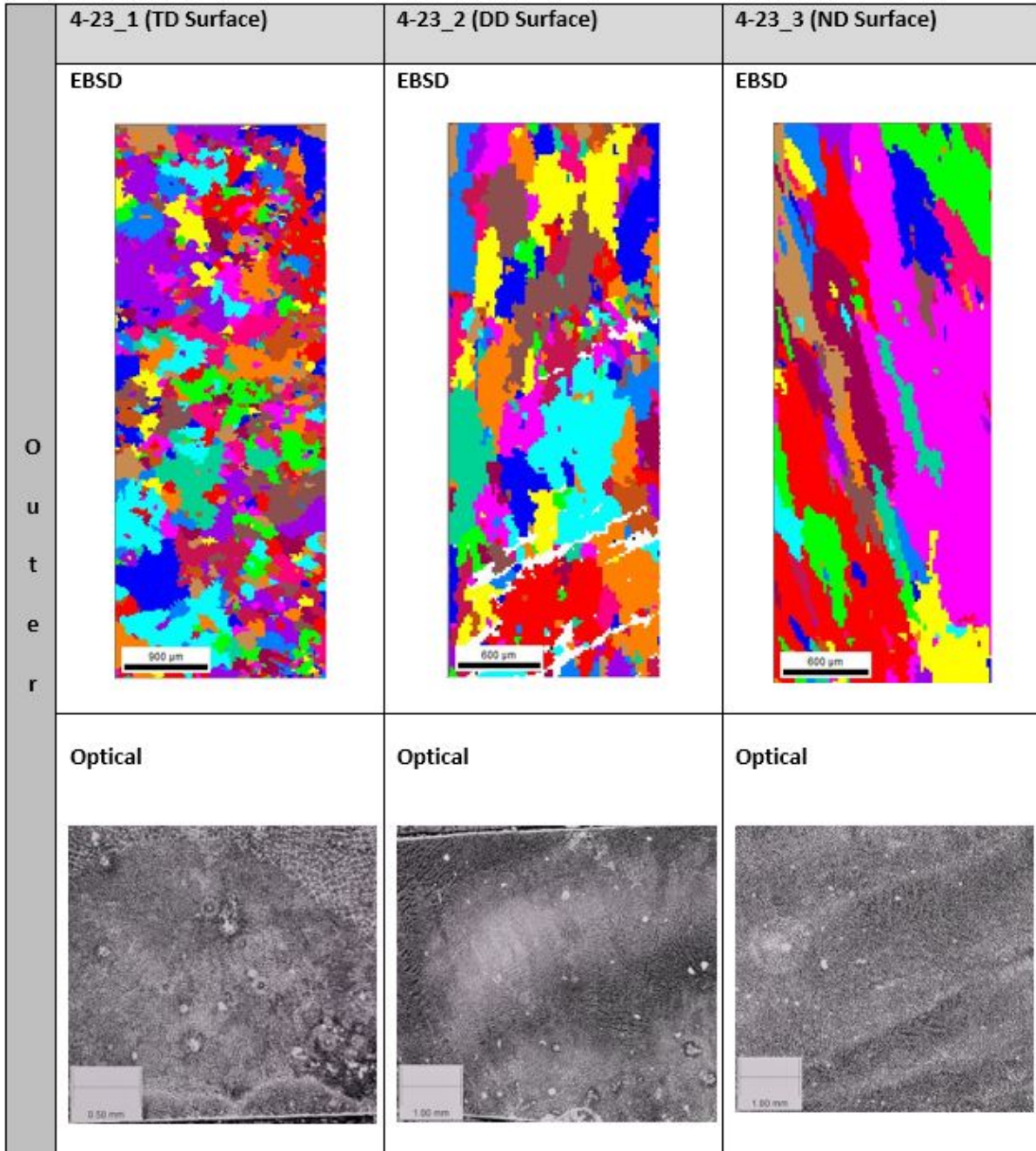


Figure 4-5: Each Surface Orientation at the Outer Plate Area

4.1.4.2 Microstructure at the Transition Zone

Figure 4-6 shows EBSD scans and optical microscopy imagery of the hot extruded plug transitioning to the EBF³ material on the ND surface of Sample 1-4. The plate's linear, columnar grains begin at the transition zone and stretch along the TD rather than along the DD, or deposition layers. Both the EBSD and optical image show there is no preference for the grains or dendrite colonies to run along the DD. Previously reviewed studies, showed preference of dendritic colonies along the DD but also documented column grains in the TD (Bird, 2010). Furthermore, columnar grains aligned to the build-up height direction and stretching across deposition layers, have been documented in other cubic metal fabricated via AM processes (Antonysamy, 2013).

Figure 4-6 also shows the bands of large and small grains that are formed as the two materials meet. This banding most likely accounts for the high amount of ductility and slight loss of strength recorded in the transition sample 1-2.

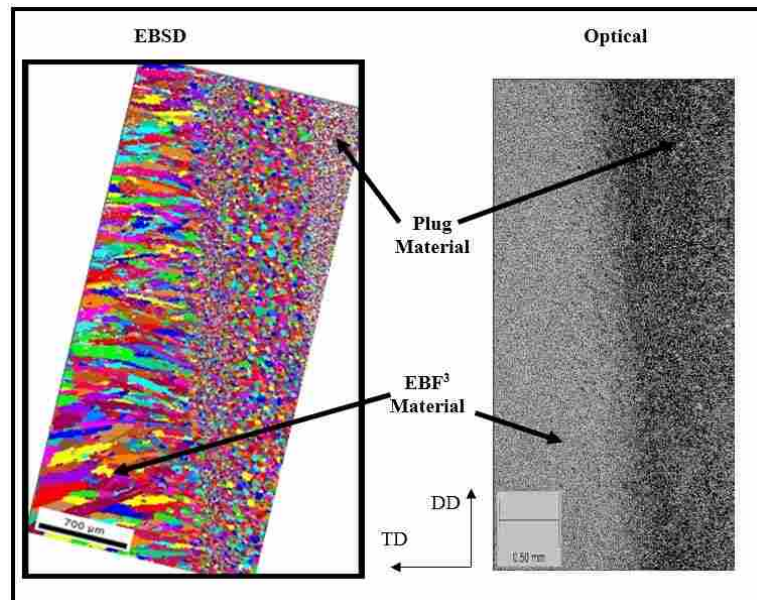


Figure 4-6: Plug to EBF³ Material on the ND Surface

4.1.4.3 Crystal Orientation

Figure 4-7 shows the crystal orientation present at each plate orientation surface and at all 15 degree increments between the DD and TD. This demonstrates that each orientation surface is inhomogeneous and textured; correlating to plate orientation direction. The ND surface is first examined starting with the plug which, since it is forged, has a homogeneous texture. At the plug to EBF³ transition area, all crystal orientations are heavily present due to the banding of large and small grains. No sample's surfaces were removed at any degree of rotation to the ND besides zero. Because of this, only one inverse pole figure is needed to represent the ND surface of the EBF³ material. The ND surface texture is oriented between each crystal orientation. The DD surface is oriented between the $\langle 110 \rangle$ and $\langle 111 \rangle$ texture. On the TD/DD surface a preference towards the $\langle 111 \rangle$ texture is observed. A strong $\langle 001 \rangle$ texture is observed on the TD surface. This differs than previously reviewed studies which documented a $\langle 001 \rangle$ texture in the DD (Tayon, 2014). However, this is most likely because previously reviewed studies recorded a layered microstructure stretch not only along the TD, but also strongly aligned the DD (Bird, 2010). As previously discussed, microstructure did not align the along the DD on the plate but rather only stretched along the TD. Furthermore, the $\langle 001 \rangle$ texture in the plate's TD is not unique because similar $\langle 001 \rangle$ textures have been observed in columnar grains aligned to the build-up height direction in other cubic metal fabricated via AM processes (Antonysamy, 2013).

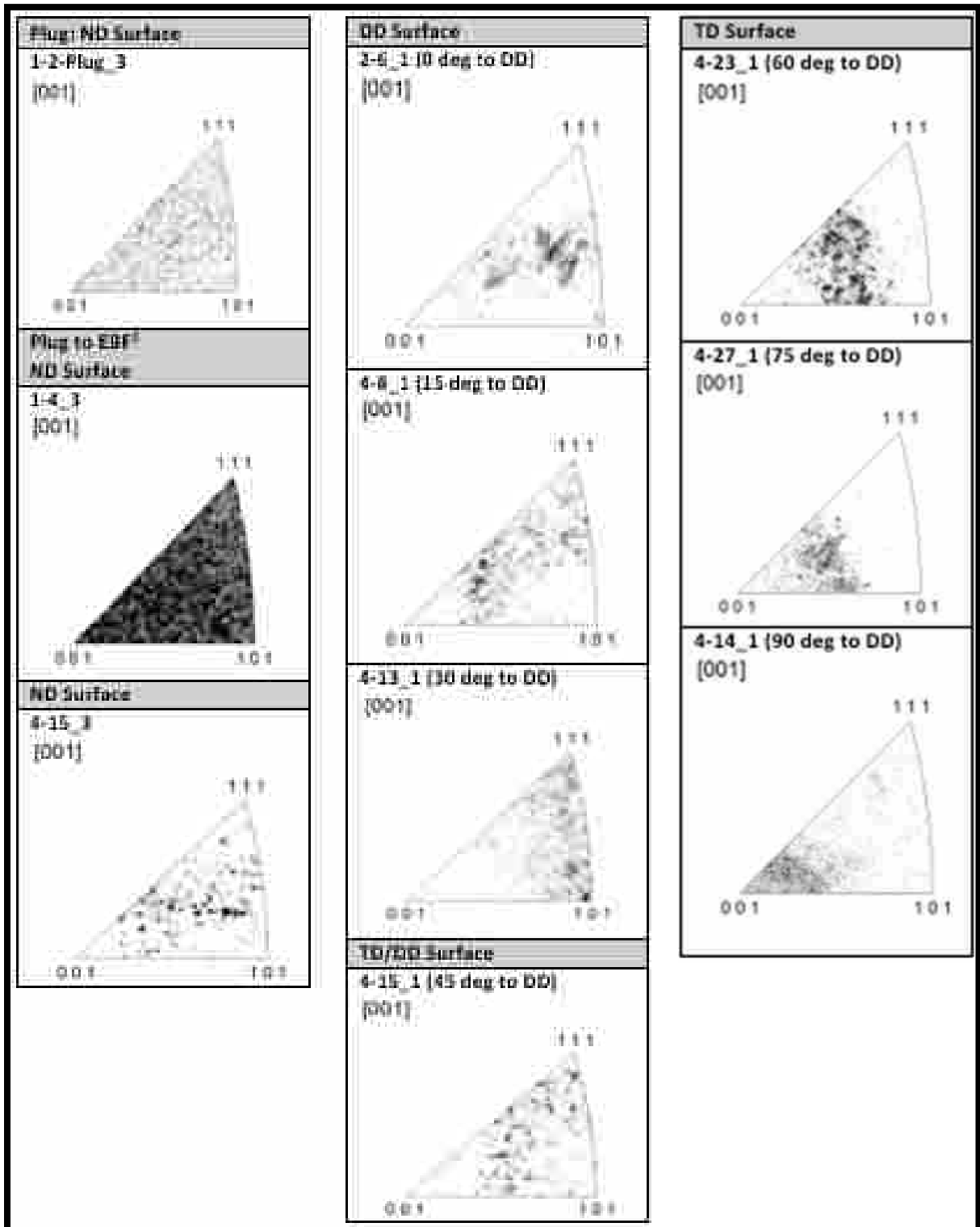


Figure 4-7: Inverse Pole Figure of Each Plate Orientation

4.1.4.3.1 Crystal Orientation Effect on Mechanical Properties

As previously discussed, the properties of nickel-base superalloys are strongly dependent on crystal orientation with the $\langle 111 \rangle$ direction having the highest strength and modulus, the $\langle 110 \rangle$ direction having the greatest ductility and the $\langle 001 \rangle$ having the lowest modulus (Dalal, 1984). Figure 4-8 shows the mechanical properties vs the degrees rotation to the DD within the ND surface plane. The strong $\langle 001 \rangle$ texture on the TD surface accounts for the low modulus and strength values recorded in TD, which is shown at 60-90 degrees to the DD. Furthermore, the high ultimate strength in the TD/DD, is shown at 30-60 degrees to the DD, can be attributed to the preference to align to the $\langle 111 \rangle$ texture.

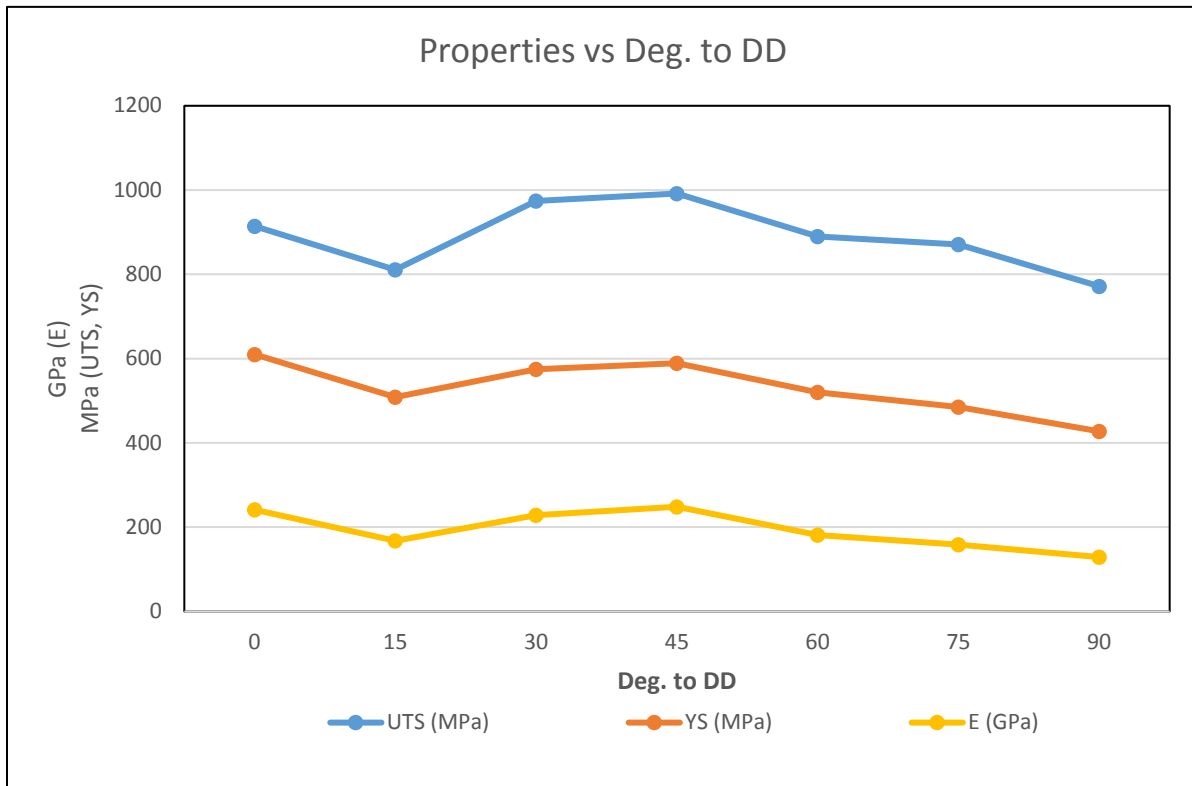


Figure 4-8: Mechanical Properties vs Degrees to DD

Figure 4-9 shows the true strain vs the degrees to the DD within the ND surface plane. The highest ductility was recorded in the DD and is represented by 0-15 degrees to the DD. The DD surface was oriented between the $\langle 110 \rangle$ and $\langle 111 \rangle$ texture. Since the $\langle 110 \rangle$ texture is associated with high ductility, this could account for the higher elongation recorded in the DD (Dalal, 1984).

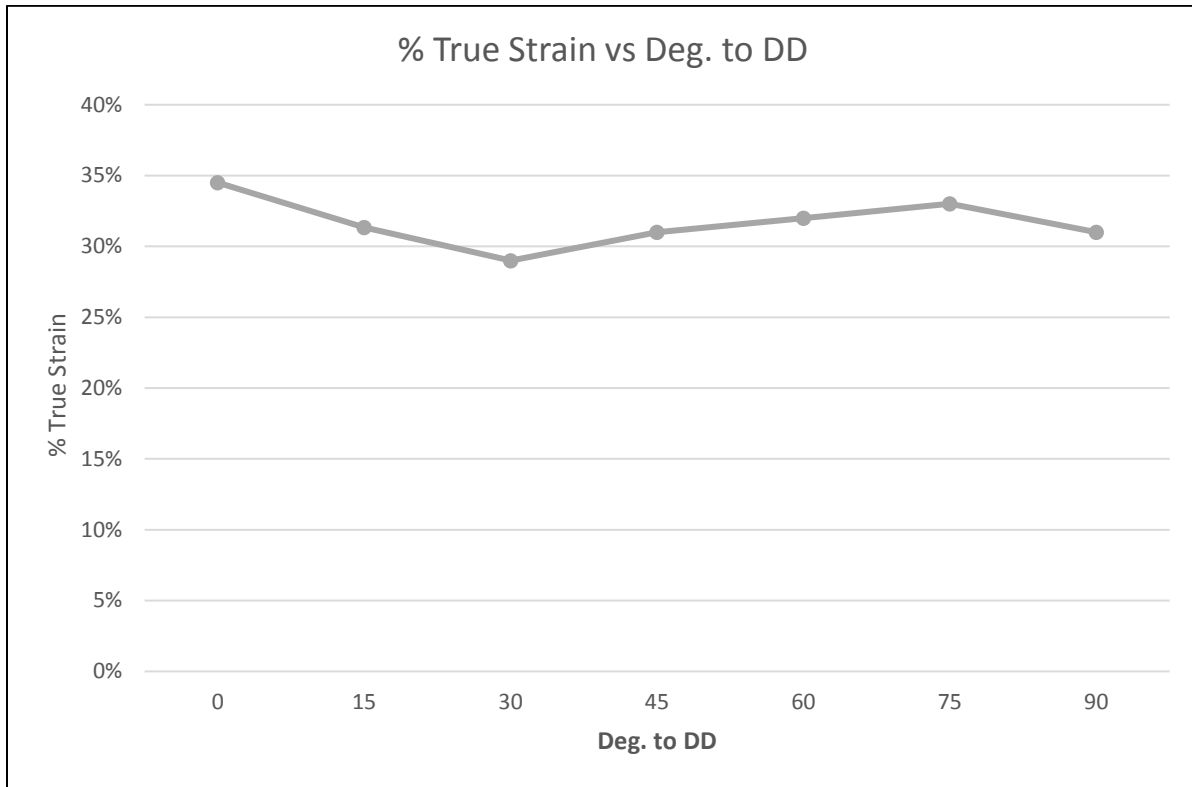


Figure 4-9: True Strain vs Degrees to DD

5 CONCLUSIONS AND RECOMMENDATIONS

5.1 H1: Height Location vs Tensile Strength

Yield strength was hypothesized to decrease higher on the build height. This hypothesis was correct and yield strength did in fact decrease along the build height. This is accounted for by the microstructure analysis which showed the changes in grain shape and size at the top area of the build height, or the outer edge of the plate. The low build height contained thin column-shaped grains, but as build height increased, the grains became wider and larger, thus reducing mechanical strength.

5.1.1 Tensile Testing

When comparing the mechanical properties' relation build height, only samples in the DD were compared because no other orientation directions were removed from both the inner and outer region of the plate. Further tensile testing needs to be conducted in the TD and ND to verify that it is not only the DD mechanical properties that are affected by build-up height. Previous studies showed that heat treatment reduced the effect of build-up height on tensile properties (Bird, 2009). Heat treatment before tensile testing needs to be conducted to verify how much the build height's effect on mechanical properties can be reduced after proper heat treatment.

5.1.2 Microscopy

The grain structure along the TD, or build-up height, started out as long and linear and broke down to wider and larger grains along the outer region of the plate. Further study needs to be conducted to try and control this phenomenon. A likely cause is the amount of cooling time allowed between each layer, since this parameter was never identified if it is significant in determining a part's properties. A study on cooling time would help determine its full effect on a part's microstructure and properties. Furthermore, heat treatment of samples needs to be conducted to document grain growth. Previous studies of heat treatment on EBF³ showed that all grains grew and became more homogenous after heat treatment (Bird, 2009). An approach that could be developed is to create the properties of heat treatment through carefully controlling the cooling time. This approach was developed for the AM technique known as electron beam melting, which utilized a IN 718 powder bed (Sames, 2015).

The grain structure typically stretched along the TD, or build height, rather than along the DD. Previous studies on NASA parts documented a layered nature of microstructure along the DD, as well as columnar grains in the TD. However, as previously reviewed in Table 2-6, the build-up height for these parts was no greater than 2 inches and long structures along the TD penetrating multiple deposition layers were only just beginning to be observed at the top of the build-up height (Bird, 2009). Most likely if these part builds continued to a higher build-up height, the microstructure along the TD would become more prevalent across deposition layers. Also, these parts had a couple minutes of cooling time before additional layers were added to them (Bird, 2009). The plate was created with a 6 inch build-up height and had almost no cooling time between layers. These factors likely allowed for the grain structure to become prevalent along the TD instead of the DD but further studies need to be conducted to verify this.

5.2 H2: Sample Orientation vs Tensile Strength

The highest yield strength was hypothesized to be in the DD since this direction doesn't pull against deposit layer interfaces. This hypothesis was correct and sample 2-6, which is oriented in the DD, demonstrated a slightly higher yield strength than the TD/DD oriented samples. This is partly due to small narrow grains in the DD, which were fully present at the low build-up height where sample 2-6 was removed. The TD/DD samples however, demonstrated a higher ultimate strength and modulus due to its alignment to the $\langle 111 \rangle$ texture. Previous studies documented a $\langle 001 \rangle$ texture in the DD along with a low DD modulus (Tayon, 2014). However, for this study, this was not the case. Rather, a $\langle 001 \rangle$ texture aligned along TD oriented columnar grains and low modulus values were recorded in the TD. These same properties were observed in other cubic metal fabricated via AM processes (Antonysamy, 2013).

5.3 Closing Remarks

This study shows that EBF³ is a viable manufacturing technique to create IN 718 parts. As previously discussed, the rotational build-up is well suited for adding EBF³ material to forged cylindrical parts. It highlights that the weakest points in the parts will be at the transition area between the two materials. During the design process, part strength requirements and limitations can be designated using this knowledge.

Furthermore, this study shows that pauses during the EBF³ process won't affect the overall strength characteristics of the part. This allows for flexible EBF³ manufacturing that is versatile and isn't time sensitive. Custom manufacturing strategies can be designed using this knowledge.

REFERENCES

- Alcisto, J., Enriquez, A., Garcia, H., Hinkson, S., Steelman, T., Silverman, E., ... & Dorey, J. (2011). Tensile properties and microstructures of laser-formed Ti-6Al-4V. *Journal of materials engineering and performance*, 20(2), 203-212.
- Antonysamy, A. A., Meyer, J., & Prangnell, P. B. (2013). Effect of build geometry on the β -grain structure and texture in additive manufacture of Ti6Al4V by selective electron beam melting. *Materials characterization*, 84, 153-168.
- ASTM, E. (2001). Standard test methods for tension testing of metallic materials, Annual book of ASTM standards. ASTM.
- Baufeld, B. (2012). Mechanical properties of Inconel 718 parts manufactured by shaped metal deposition (SMD). *Journal of materials engineering and performance*, 21(7), 1416-1421.
- Benn, R. C., Salva, R. P., & Engineering, P. (2010). Additively Manufactured INCONEL (®) Alloy 718. *TMS Superalloy 718 and Derivatives Proceedings*, 7th, 455-69.
- Bird, R. K., & Atherton, T. S. (2010). Effect of Orientation on Tensile Properties of Inconel 718 Block Fabricated with Electron Beam Freeform Fabrication (EBF3).
- Bird, R. K., & Hibberd, J. (2009). Tensile Properties and Microstructure of Inconel 718 Fabricated with Electron Beam Freeform Fabrication (EBF (sup 3)).
- Brown, W. F., Ho, C. Y., & Mindlin, H. (1979). *Aerospace structural metals handbook*. CINDAS-USAF CRDA Handbooks Operation, Purdue University. Vol. 6, Code 4103.
- Da Silveira, G., Borenstein, D., & Fogliatto, F. S. (2001). Mass customization: Literature review and research directions. *International journal of production economics*, 72(1), 1-13.
- Dalal, R. P., Thomas, C. R., & Dardi, L. E. (1984). The effect of crystallographic orientation on the physical and mechanical properties of an investment cast single crystal nickel-base superalloy. *Superalloys*, 84, 185-197.
- Dieter, G. E., & Bacon, D. J. (1986). *Mechanical metallurgy* (Vol. 3). New York: McGraw-hill.
- Frazier, W. E. (2014). Metal additive manufacturing: a review. *Journal of Materials Engineering and Performance*, 23(6), 1917-1928.

- Handbook—Volume, A. S. M. (2005). 6, Code 4103. *Brown, Mindlin, and Ho, eds, 39.*
- Lingenfelter, A. (1989). Welding of Inconel alloy 718: A historical overview. *Superalloy, 718*, 673-683.
- Paulonis, D. F., & Schirra, J. J. (2001). Alloy 718 at Pratt&Whitney—historical perspective and future challenges. *Superalloys, 718(625,706)*, 13-23.
- Ram, G. J., Reddy, A. V., Rao, K. P., & Reddy, G. M. (2005). Microstructure and mechanical properties of Inconel 718 electron beam welds. *Materials science and technology, 21(10)*, 1132-1138.
- Reed, R. C. (2008). *The superalloys: fundamentals and applications*. Cambridge university press.
- Ruan, J., Sparks, T. E., Fan, Z., Stroble, J. K., Panackal, A., & Liou, F. (2006). A review of layer based manufacturing processes for metals. In *17th Solid Freeform Fabrication Symposium, Austin (USA)* (pp. 233-245).
- Ruff, P. E., (1986). Effect of Manufacturing Processes on Structural Allowables— Phase I: *Air Force Wright Aeronautical Laboratories*, Technical Report No. AFWAL-TR-85-4128.
- Standard, A. S. T. M. (2004). E8-04, “*Standard Test Methods for Tension Testing of Metallic Materials,*” Annual Book of ASTM Standards. Vol. 03.01.
- Sames, W. (2015). *Additive manufacturing of Inconel 718 using electron beam melting: Processing, post-processing, & Mechanical properties* (Doctoral dissertation).
- Taminger, K. M. (2008). Electron beam freeform fabrication: a fabrication process that revolutionizes aircraft structural designs and spacecraft supportability.
- Taminger, K. M., & Hafley, R. A. (2006). Electron beam freeform fabrication for cost effective near-net shape manufacturing.
- Tayon, W. A., Shenoy, R. N., Redding, M. R., Bird, R. K., & Hafley, R. A. (2014). Correlation Between Microstructure and Mechanical Properties in an Inconel 718 Deposit Produced Via Electron Beam Freeform Fabrication. *Journal of Manufacturing Science and Engineering, 136(6)*, 061005.
- U.S. Department of Defense, (1999). Military Handbook—MIL-HDBK-5H: *Metallic Materials and Elements for Aerospace Vehicle Structures*, Washington, DC.
- Wohlers, T., & Gornet, T. (2011). History of additive manufacturing. *Wohlers Report: Additive Manufacturing and 3D Printing State of the Industry Annual Worldwide Progress Report*.